



Norwegian University of
Science and Technology

Advanced Probabilistic Slope Stability Analysis on Rissa Slope

Amanuel Petros Wolebo

Geotechnics and Geohazards

Submission date: June 2016

Supervisor: Gudmund Reidar Eiksund, BAT

Co-supervisor: Ivan Depina, IGB

Norwegian University of Science and Technology
Department of Civil and Transport Engineering



Report Title: Advanced Probabilistic Slope Stability Analysis on Rissa Slope	Date: 10.06.2016			
	Number of pages: 95			
	Master Thesis	X	Project Work	
Name: Amanuel Petros Wolebo				
Professor in charge/supervisor: Professor Gudmund Reidar Eiksund, BAT				
Other external professional contacts/supervisors: PhD. Candidate Ivan Depina, IGB				

<p>Abstract</p> <p>Uncertainties on different soil properties affect the reliability of geotechnical analysis. In geotechnical design the most adopted procedure to account for uncertainty is, to maintain some degree of safety by using characteristic values and factor of safety approaches. This method does not give a complete indication of safety margin. Too high safety standards cause expensive system, whereas too low factor of safety results many casualty and economic damage. How the uncertainties in soil parameters affect the geotechnical reliability analysis should be dealt adequately and the uncertainties should be quantified and carefully evaluated.</p> <p>This thesis focuses on the evaluation of the effect of uncertainty and soil variability on stability analysis within the formwork of probabilistic methods and contributes to the application of advanced probabilistic method in geotechnical slope stability analysis. Conditional random finite element method (CRFEM) creates a computational model able to estimate the probability of failure of a slope while fully accounting for for spatial variability of soil. The applicability of CRFEM shows the potential of the framework of uncertainty quantification and the effects of soil variability and spatial variability at different scales on the studied case.</p> <p>The case study is based on the ground investigation made while planning a road project in Rissa area located in Sør-Trøndelag, Norway. The area is famous for the quick clay slide that occurred in 1978.</p>
--

Keywords:

1. Uncertainty
2. Spatial variability
3. Slope stability
4. CRFEM

Amanuel Petros Wolebo

Foreword

This Master thesis is submitted for the fulfillment of Master of Science degree (MSc) in Geotechnics and Geohazard program at the Norwegian University of Science and Technology. The thesis was written over a course of 20 weeks, Spring 2016. In this study, advanced probabilistic slope stability analysis is conducted on Rissa Slope based on probabilistically interpreted soil parameters from CPT data, accounting for spatial variability of soil. The idea behind this study was raised by PhD. Candidate Ivan Depina.

Trondheim, 2016

Acknowledgments

First and foremost, I would like to thank God. I could not have done this without the faith I have in you. “For you are my hiding place; you protect me from trouble. You surround me with songs of victory.”

I am very grateful to my Families. Their unconditional love and encouragement supported me to pursue my dreams. They will stay being the most important persons in my life and I do love them deeply. In particular, I would like to thank my uncle, Feleke Bekele and my brother, Simon Petros for covering all my expenses during my studies and for their invaluable advice. This could never have happened without their support.

I would like to express my deep gratitude to my supervisor, Ivan Depina for his extensive and priceless guidance, for his constant support and patience, for sharing his knowledge and experience, throughout my MSc studies despite his busy schedule.

Likewise, I thank Prof. Gudmund Reidar Eiksund and Prof. Vikas Thakur for their expert advice and feedback throughout the time of my studies.

Amanuel Petros
Trondheim, June 2016

Summary

The core competence of a civil engineer is developing reliable and effective systems for the society by mitigating risk and reducing failure. This includes forecasting and prevention against catastrophes due to natural hazards. Natural hazards cause significant damage on human life and economic loss. To minimize these enormous amount of damages, especially caused by geohazards, an appropriate preventing techniques are needed and reliability analysis relating geohazards should be adopted.

Uncertainties on different soil properties affect the reliability of geotechnical analysis. In geotechnical design, the most adopted procedure to account for uncertainty is to maintain some degree of safety by using characteristic values and factor of safety approaches. This method does not give a complete indication of safety margin and is unable to properly characterize spatial variability. Too high safety standards cause expensive system, whereas too low factor of safety results many casualty and economic damage. Therefore, how the uncertainties in soil parameters affect the geotechnical reliability analysis should be dealt adequately and the uncertainties should be quantified properly. Quantifying the uncertainties in geotechnical engineering subjected to inherent randomness in properties is becoming increasingly important, and the implementation of more advanced and sophisticated techniques to ensure proper safety standards for society is becoming essential.

This thesis focuses on the evaluation of the effect of soil variability within the formwork of probabilistic methods and contributes to the application of advanced probabilistic method in geotechnical slope stability analysis. Advanced probabilistic analysis method provides a means to quantify the reliability of complex systems. The integration between probability concept (conditional random field) and a numerical technique, Finite Element Method (FEM) created a powerful analysis method called Conditional Random Finite Element Method (CRFEM). CRFEM creates a computational model that is able to estimate the probability of failure of a slope while fully accounting for spatial variability of soil. A

case study, Rissa slope demonstrates the applicability of CRFEM approach and shows the potential of the framework on uncertainty quantification and the effects of soil variability and spatial variability at different scales.

This thesis is structured thematically in the following parts:

Chapter 2: The background information concerning the basic statistic terms such as, random variable, continuous probability distributions and brief explanation on cone penetration testing are presented.

Chapter 3: This chapter focuses on the basics of soil variability and safety. It provides a description on source of uncertainties and common approaches for dealing with soil variabilities. The basics of generation of random numbers and conditional random field are included. Moreover, an introduction into slope stability and probabilistic analysis method are given.

Chapter 4: This chapter briefly describes the studied case, Rissa area. Background information and the famous quick clay land slide appeared on this area are presented. It also explains the ground investigations made, the challenges faced during planning of a road project and the cause for the termination the planned project which is the main initiative for this study.

Chapter 5: This chapter presents the application of statistics from chapter 3 on the available data described in chapter 4. The applied method in estimation of soil variability and the proceeding probabilistic interpretation of soil parameters from the available data, CPT is provided clearly.

Chapter 6: The results followed by the application of Conditional Random Finite Element Method based on the outcomes of chapter 5 as an input is described. A number of different simulations used to analyze the effect of soil variability and spatial variability is presented in detail.

Chapter 7: The outline for the overall procedure and brief discussion about the results identified in chapter 5 and chapter 6 are presented.

Chapter 8: In this chapter, conclusion is drawn on the achievement of the whole project. A summary of the objectives of this thesis and finally, recommendations for further work is proposed.

Contents

FOREWORD	III
ACKNOWLEDGMENTS	V
SUMMARY	VII
NOMENCLATURE	XVII
1 INTRODUCTION	1
1.1 BACKGROUND AND RATIONALE	1
1.2 PROBLEM FORMULATION.....	2
1.3 RESEARCH AIM	2
1.4 STRUCTURE OF THE REPORT	3
2 THEORETICAL FOUNDATION	5
2.1 BASICS OF PROBABILITY	5
2.1.1 <i>Random variable</i>	5
2.1.2 <i>Measure of central tendency and variability</i>	6
2.1.3 <i>Continuous probability distributions</i>	7
2.2 CONE PENETRATION TESTING	9
2.2.1 <i>Cone tip resistance</i>	10
3 SOIL VARIABILITY AND SAFETY	13
3.1 SOIL VARIABILITY	13
3.1.1 <i>Uncertainty</i>	13
3.1.2 <i>Trend analysis</i>	14
3.1.3 <i>Local average</i>	15
3.2 RANDOM FIELD	16
3.2.1 <i>Gaussian random field</i>	16
3.2.2 <i>Autocorrelation and correlation length</i>	17
3.2.3 <i>Conditional Gaussian random field</i>	18

3.2.4	<i>Generating random field</i>	19
3.3	SLOPE STABILITY	19
3.3.1	<i>Factor of safety</i>	19
3.3.2	<i>Probabilistic slope stability method</i>	21
3.3.3	<i>Monte Carlo sampling technique</i>	21
4	DESCRIPTION OF RISSA AREA	23
4.1	RISSA LANDSLIDE	23
4.2	BACKGROUND INFORMATION.....	24
4.3	GROUND INVESTIGATIONS.....	25
5	PROBABILISTIC INTERPRETATION OF SOIL PARAMETERS	
	FROM CPT	27
5.1	ESTIMATION OF CORRELATION LENGTH.....	27
5.1.1	<i>Maximum likelihood estimation</i>	27
5.2	PROBABILISTIC INTERPRETATION OF SHEAR STRENGTH OF SOIL	31
5.2.1	<i>Undrained shear strength</i>	31
5.2.2	<i>Friction angle</i>	36
6	RESULTS	41
6.1	SLOPE STABILITY ANALYSIS	41
6.2	DETERMINISTIC SLOPE STABILITY METHOD	41
6.3	SINGLE RANDOM VARIABLE METHOD	43
6.4	CONDITIONAL RANDOM FINITE ELEMENT METHOD.....	45
6.4.1	<i>Generating Mesh</i>	45
6.4.2	<i>Spatial Length</i>	46
6.4.3	<i>CoV of unobserved elements</i>	46
6.4.4	<i>Local averaging of elements</i>	47
6.5	SIMULATION RESULTS	49
6.5.1	<i>Probability of failure</i>	52
6.5.2	<i>The effect of CoV</i>	54
6.5.3	<i>The effect of horizontal correlation length</i>	55
6.5.4	<i>Effect of local averaging</i>	56
7	DISCUSSIONS	59
7.1	UNCERTAINTY AND PARAMETERS INTERPRETATION	60

7.1.1	<i>Spatial variability</i>	60
7.1.2	<i>Probabilistic interpretation of parameters</i>	60
7.2	CONDITIONAL RANDOM FIELD.....	61
7.2.1	<i>Monte Carlo sampling</i>	62
7.3	FACTOR OF SAFETY AND FAILURE PROBABILITY.....	63
8	CONCLUSIONS AND RECOMMENDATIONS	67
8.1	CONCLUSIONS.....	67
8.2	RECOMMENDATIONS FOR FURTHER WORK.....	68
	BIBLIOGRAPHY	71

List of Tables

3.1	Factor of safety criteria from U.S Army Corps of Engineers' slope stability manual	20
4.1	Soil layering and ground water depth of CPT profiles	26
5.1	Maximum likelihood estimation result for $\theta_{\ln qt}$, $\mu_{\ln qt}$, and $\sigma_{\ln qt}^2$ for all profiles.....	30
5.2	Input values of parameters used for probabilistic interpretation of S_u of clay layers of profile C4.....	33
5.3	Input values of parameters parameters used for probabilistic interpretation of φ of sand layer of profile C4.....	39
6.1	Plaxis 2D deterministic input parameters	42
6.2	Plaxis 2D input values of parameters for single random variable approach.....	43
6.3	Position and weight factor of 12-point integration for 15 - node elements.....	48
6.4	Input values of parameters for unobserved points for simulation 1.....	48
6.5	Input parameters of unobserved points for all simulations given in terms of simulation 1	49
6.6	Mean value for F_s and probability of failure for simulation 1-7.....	54
7.1	Comparison between deterministic, SRV and CRFEM approaches.....	63

List of Figures

2.1	Probability density plot of normal distribution with $\mu = 5$ and $\sigma = 2$	7
2.2	Probability density plot of lognormal distribution with $\mu = 5$ and $\sigma = 2$	8
2.3	Probability density plot of generalized extreme value distribution with $\mu = 5, \sigma = 2$ and $k = -0.5$	9
2.4	Schematic of Piezocone (CPTU) picture taken from (Craig, 2004).....	10
3.1	Two data having same mean and standard deviation, but different pattern of spatial variation. Picture taken from (Baecher & Christian, 2005).....	15
4.1	Rissa landslide occurred on 29 April, 1978	23
4.2	Aerial Photography map of Rissa showing the planned road alignmnet (Google Maps).....	24
4.3	Geometry, soil layering and CPT profile points of Rissa slope, section 3-3 profile C.....	26
5.1	Log-likelihood function for a range of correlation lengths, $\theta \ln q$ for C4	29
5.2	Mean value of S_u with 90% confidence interval for profile C4 clay layers.....	36
5.3	Computed values of ϕ using Eq. 5.21 and Eq. 5.22 with the fitted regression model having a form as Eq.5.23	38
5.4	Mean value of ϕ with 90% confidence interval for profile C4, sand layer	40
6.1	Plaxis 2D input Geometry of Rissa Slope.....	42
6.2	Failure mechanism of the slope in terms of deviatoric strain	42
6.3	Histogram plot and distribution fit of F_s for 2000 MC realizations.....	44
6.4	Cumulative density function of F_s showing 30.1% probability of failure	45
6.5	Generated mesh diagram with boundary box surrounding CPT profiles	46

6.6	Local numbering and positioning of nodes of a 15 - node triangular element ...	47
6.7	Plaxis 2D geometry output of generated random field for simulation 1.....	50
6.8	Deformed mesh output at the end of elastic analysis.....	50
6.9	Failure mechanism in terms of deviatoric strain for simulation 1	50
6.10	Histogram plot and distribution fit of F_s for 1000MC realizations for simulation 2 (a) and simulation 3 (b).....	51
6.11	Failure probability realization including the effect of model uncertainty for simulation 2 ($CoV = 1.5 CoV1$).....	53
6.12	Failure probability realization including the effect of model uncertainty for simulation 3 ($CoV = 2 CoV1$).....	53
6.13	The effect of CoV on F_s and p_f for simulations 1, 2 and 3	55
6.14	The effect of horizontal correlation length on F_s and p_f for simulations 4, 5 and 6 ($\theta_H = 1m, 15m$ and $100m$ respectively).....	55
6.15	The effect of local averaging, simulation 7 on F_s and p_f implemented on simulation 3.....	56
7.1	Overall procedure for application of advanced probabilistic slope stability analysis.....	59
7.2	Conditionality effect on the generated random field for simulation 3.....	61
7.3	Relation between coefficient of variation and probability of failure.....	64
7.4	Relation between horizontal correlation length and probability of failure	64

Nomenclature

Latin Symbols

a	Net area ratio
a	Attraction
A	Lower triangular matrix
A^T	Upper triangular field
A_q	Projected area of cone
A_n	Cross sectional area of load cell
B_q	Pore pressure ratio
C	Covariance matrix
CoV	Coefficient of variation
Cov	Covariance
E	Expectation
f_x	Probability density function
f_{xy}	Joint bivariate function
F_s	Factor of safety
g	Performance function
I_p	Plasticity index
k	Shape factor
\mathcal{L}	Log-likelihood function
L	Likelihood function
LN	Lognormal distribution

N	Normal distribution
N_{kt}	Empirical cone factor
N_s	Number of realization
OCR	Overconsolidation ratio
p_f	probability of failure
q_c	Cone tip resistance
q_t	Corrected cone resistance
R	Random field realization
S_t	Sensitivity
S_u	Undrained shear strength
u	Residual
u_2	Total pore pressure in cone joint
X	Random variable
z	Depth

Greek symbols

β	Plastification angle
γ	Soil unit weight
ϵ_q	Measurement error
ϵ_M	Model error
ϵ_R	Regression model error
ϵ_T	Transformation error
θ	Correlation length
μ	Mean
ρ	Correlation coefficient

σ	Standard deviation
σ_{vo}	Total overburden stress
σ'_{vo}	Effective overburden stress
τ	Distance
τ_f	Shear strength of soil
τ_{mob}	Mobilized shear stress
Φ	Standard normal cumulative density function
φ	Friction angle

Abbreviations

CPT	Cone Penetration Test
CPTU	Cone Penetration Test with pore pressure
CRFEM	Conditional Random Finite Element Method
MLE	Maximum likelihood estimation
NGI	Norwegian Geotechnical Institution
NGU	Geological survey of Norway
NPRA	Norwegian Public Road Administration
SRV	Single Random Value

Chapter 1

Introduction

1.1 Background and rationale

The core competence of a civil engineer is developing reliable and effective systems for the society by mitigating risk and reducing failure. This includes forecasting and prevention against catastrophes due to natural hazards. According to a 2014 report by the United Nations, since 1994, natural disasters caused around USD 2 trillion economic damage world wide and affected more than 4 billion people (Kellet, 2014). To minimize these enormous amount of damages, especially caused by geohazards, an appropriate preventing techniques are needed. The assessment, prevention and mitigation methods of geohazards, including risk associated with landslide and mass transport in soil due to flooding, and earthquakes should take one step further and implement more advanced and sophisticated techniques to ensure proper safety standards for society.

In deterministic geotechnical design, global and partial factor of safety concepts are commonly used to maintain some degree of safety, mainly driven by expert judgement or experience. There is no standard measure for factor of safety due to the variability and uncertainty of natural phenomenon. Too high safety standards cause expensive system, whereas too low factor of safety results many casualty and economic damage. How to properly handle variability and uncertainty of nature is challenging task, and as described by Fenton and Griffiths, “*We will never know the precise distribution of any natural phenomenon. Nature cares not at all about our mathematical models and the truth is usually far more complex than we are able to present*” (Fenton & Griffiths, 2008c). Therefore, an advanced

method is necessary for evaluating safety of structures by considering variability and uncertainty in a proper way. One of the techniques is the implementation of advanced probabilistic slope stability analysis on factor of safety concept. This helps geotechnical engineers to analyze the impact of hazards on structures and also for making an economical and safe design approach.

1.2 Problem formulation

In geotechnical engineering, evaluation of land slide hazards and slope stability analysis are still carried out in a deterministic framework based on experience. The determined factor of safety does not give any information on failure occurrence probability. Especially in assessing regional land slide risks, estimation of the probability of slope failure during some specific period of time is the most basic. Therefore, this study put the emphasis to examine factor of safety and failure probability by implementing advanced probabilistic analysis method.

How to quantify uncertainty and variability of soil parameters, probabilistic interpretation of soil properties from CPT measurement, how to incorporate a number of observations of CPT profiles in slope stability analysis, the interaction between unobserved and observed points within a slope geometry are the basic concepts dealt in this thesis by taking a specific case study on Rissa Slope.

1.3 Research aim

This paper is focusing on evaluation of the effect of soil variability and uncertainty on stability analysis within the formwork of probabilistic methods. Application of probabilistic analysis by sampling techniques on real case, Rissa Slope, and discovering the inherent relationship between soil shear strength parameters (undrained shear strength and friction angle) with failure probability is the main intention. To achieve this aim, several topics on theory of geostatistics, random field and uncertainties due to interpretation of CPT are studied widely.

1.4 Structure of the report

In addition to this introduction section, the thesis is arranged in seven chapters as indicated below:

At first an introduction to background information is given in **Chapter 2**. This includes recognizing basic statistic terms such as random variable, continuous probability distributions and brief explanation on cone penetration testing are presented. The basics of soil variability and safety within **Chapter 3** provides a description on source of uncertainties and common approaches for dealing with soil variabilities. The basics of generation of random numbers and conditional random field are included. Moreover, an introduction into slope stability and probabilistic analysis method are provided.

Chapter 4 briefly describes the studied case, Rissa area. The background information and the famous quick clay land slide appeared on this area are presented. The ground investigations that are made several times are briefly stated.

In **Chapter 5**, a specific method for estimation of soil variability and the proceeding probabilistic interpretation of soil parameters form the available CPT measurement data are provided clearly.

Chapter 6 presents the application of Conditional Random Finite Element Method on Rissa slope based on the preceding outcomes of chapter 5. A number of different simulations used to analyze the effect of spatial soil variability are presented in detail.

Chapter 7 gives the outline for the overall procedure and brief discussions are provided about the results identified in chapter 5 and chapter 6.

Chapter 8 is a summary of the objectives of this thesis. Finally, recommendations for further work is proposed.

All calculations regarding estimation of soil variability and probabilistic interpretation of soil parameters are performed by using MATLAB® R2015b, mesh generation for CRFEM is adapted by a software, GMSH 2.12, and simulations with sampling techniques are made by interacting a programming language, Python (xy) with the finite element software, PLAXIS 2D

Chapter 2

Theoretical foundation

2.1 Basics of Probability

The main concern of this thesis, advanced probabilistic slope stability analysis, is the outcome of a combined effect of simple and basic statistics. Therefore, it is inevitable to recall some basic knowledge concerning probabilistic theory. The basic statistics terms mentioned in this chapter are applied in this study and worth describing them briefly.

2.1.1 Random variable

A random variable is a variable that is subject to randomness, which can take numerical values by the outcome of some chance process. The definition given by ISSMGE technical committee on risk assessment and management is: “*a quantity, the magnitude of which is not exactly fixed but rather the quantity may assume any of the number of values described by a probability distribution*”(ISSMGETC32, July, 2004). A random variable can be either discrete or continuous.

A discrete random variable is a variable that represent numbers found by counting. It has countable set of outcomes and takes fixed set of possible value like number of blows in a standard penetration test. The probability distribution gives the possible values of the variables and their probability.

Continuous random variables are random variables that are found from measuring and take values in an interval or on continuous scale such as, the values of undrained shear

strength of clay. The probability distribution is described by a density curve and the probability of an event is the corresponding area under the curve.

2.1.2 Measure of central tendency and variability

Random variables can be described by using easy estimated measures. The most important of these measures are central tendency (mean) and variability (standard deviation). These quantities convey information about the properties of random variable that are of first importance in practical application (Fenton & Griffiths, 2008a).

Mean or expected value is a measure of central tendency of random variable or probability distribution. For a given sample x , the mean value, μ_x is computed as the sum of all the observed outcomes from the sample divided by the total number of events, N .

$$\mu_x = E(x) = \frac{1}{N} \sum_{i=1}^n x_i \quad (2.1)$$

Standard Deviation is a measure of dispersion or how spread the set of data values are. A standard deviation close to zero, indicates that the data points tend to be very close to the mean value of the data set, while a high standard deviation indicates that the data points are spread out over a wider range of values. Sample standard deviation, σ_x of the population based on a set of observation x_1, x_2, \dots, x_n is calculated by:

$$\sigma_x = \sqrt{E(x - \mu_x)^2} = \sqrt{\frac{1}{N} \sum_{i=1}^n (x_i - \mu_x)^2} \quad (2.2)$$

The variability of a random quantity is often expressed using dimensionless measures called **coefficient of variation**, CoV which is a ratio of standard deviation over mean.

$$CoV_x = \frac{\sigma_x}{\mu_x} \quad (2.3)$$

2.1.3 Continuous probability distributions

There are several models that describe the distribution of random variables. Values of soil parameters identified by measurement take values in interval scale. These continuous random variables of soil parameters are represented by continuous probability distributions and the equation used to describe is called probability density function. In this study, the continuous models used to represent soil characterizations are explained briefly.

Normal distribution is the most important continuous distribution in use today. This is because the whole distribution can be defined completely with only the first two moments, mean and standard deviation. Central limit theorem shows that the sums of random variables tend to follow a normal distribution (Dudley, 1999). Since many natural phenomena involve many accumulating factors, they tend to have normal distribution. Normal distribution is symmetric about the mean, which is also the maximum point of the distribution as shown in Fig. 2.1. A random variable X follows a normal distribution if its probability density function has the form:

$$f_x(x) = \frac{1}{\sigma\sqrt{2\pi}} \exp \left\{ -\frac{1}{2} \left(\frac{x-\mu}{\sigma} \right)^2 \right\}; \quad -\infty < x < \infty \quad (2.4)$$

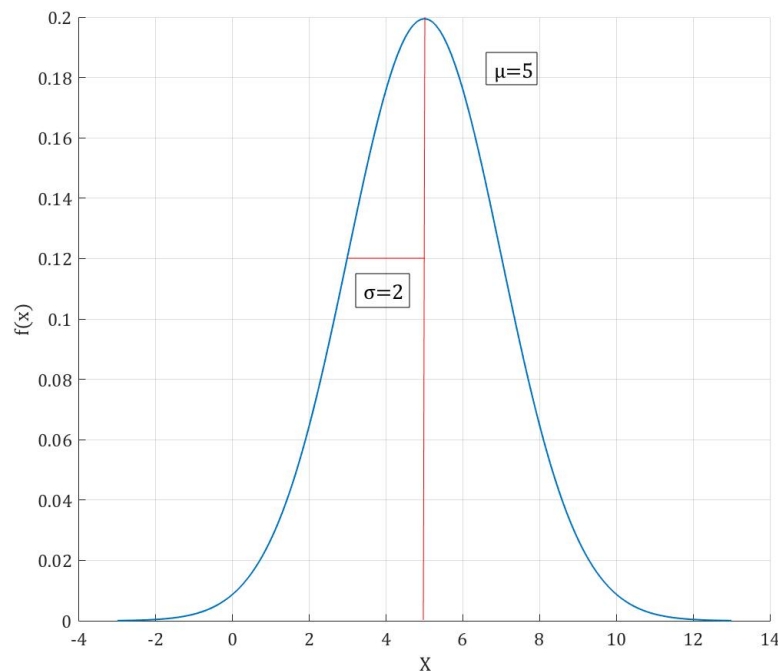


Figure 2.1 Probability density plot of normal distribution with $\mu = 5$ and $\sigma = 2$

Lognormal distribution

A continuous variable tends to follow a lognormal distribution, if the variable is a product of a large number of independent, identically distributed variables as proven by central limit theorem (Dudley, 1999). A random variable will follow a lognormal distribution if the logarithm of the variable is a normally distributed random variable. Thus, if the random variable X is lognormally distributed, then $Y = \ln X$ is normally distributed. Likewise, if Y has a normal distribution with range $-\infty < Y < \infty$, then $X = \exp(Y)$ is lognormally distributed with a range of $0 \leq X < \infty$. A random variable that is lognormally distributed takes only positive real values as shown in Fig. 2.2. The probability density function for lognormal distribution is given by:

$$f_x(x) = \frac{1}{x\sigma_{\ln x}\sqrt{2\pi}} \exp\left\{-\frac{1}{2}\left(\frac{\ln x - \mu_{\ln x}}{\sigma_{\ln x}}\right)^2\right\}; \quad 0 \leq x < \infty \quad (2.5)$$

Where, $\mu_{\ln x}$ and $\sigma_{\ln x}$ are the mean and standard deviation of the underlying normally distributed random variable, $\ln x$ and given by:

$$\sigma_{\ln x} = \sqrt{\ln\left[1 + \left(\frac{\sigma_x}{\mu_x}\right)^2\right]} \quad ; \quad \mu_{\ln x} = \ln(\mu_x) - \frac{\sigma_{\ln x}^2}{2} \quad (2.6)$$

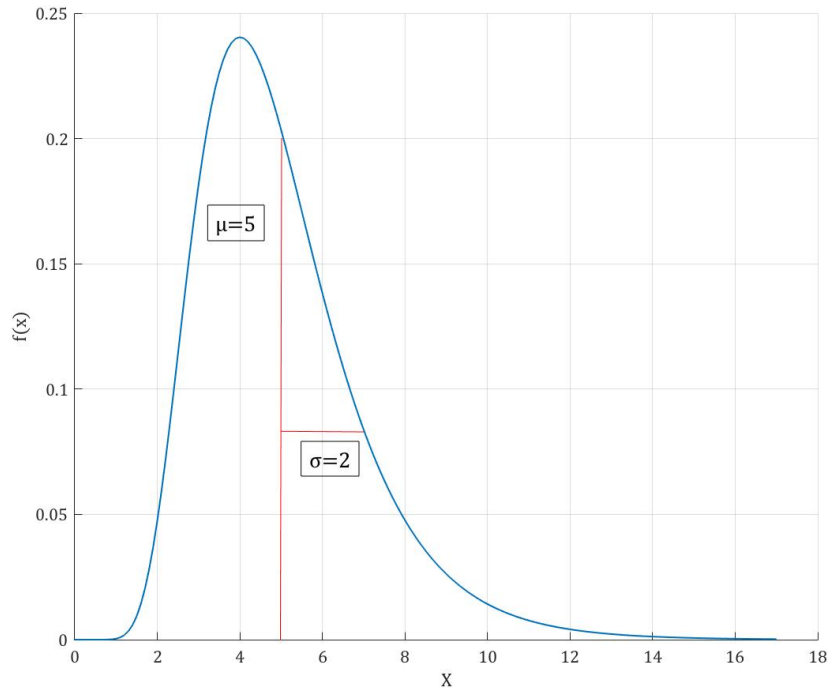


Figure 2.2 Probability density plot of lognormal distribution with $\mu = 5$ and $\sigma = 2$

Generalized extreme value distribution

Generalized extreme value distribution is one of the continuous probability distribution used to model extreme events. It is a model that combines Gumbel and Weibull maximum extreme value distribution. The probability density function for generalized extreme value distribution with location parameter, μ scale parameter, σ and shape parameter, $k \neq 0$ is given by:

$$f_x(x) = \frac{1}{\sigma} \exp \left(- \left(1 + k \frac{(x - \mu)}{\sigma} \right)^{\frac{-1}{k}} \right) \left(1 + k \frac{(x - \mu)}{\sigma} \right)^{-1 - \frac{1}{k}} \quad (2.7)$$

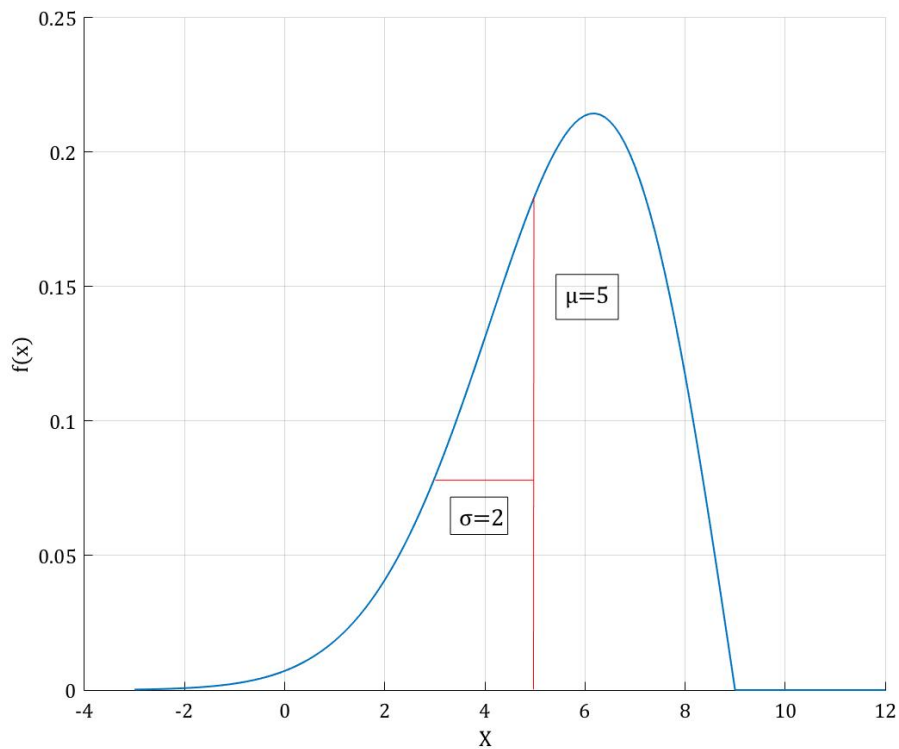


Figure 2.3 Probability density plot of generalized extreme value distribution with $\mu = 5$, $\sigma = 2$ and $k = -0.5$

2.2 Cone penetration testing

Cone penetration testing (CPT) permits rapid exploration of subsurface conditions while minimizing retrieval of subsurface material. This exploration method employs sensors that are pushed into the ground to infer the properties of both soils and pore fluids (Noce, 2003). The test method consists of pushing an instrument cone into the ground at a controlled rate.

While penetrating the ground with a constant rate, a continuous real time measurement of cone resistance, q_c and sleeve friction, f_c is recorded. CPTU is an improved CPT with capability of excess pore water pressure measurement behind the cone, u_2 and is more suited for measuring fine grained soils like clay. Figure 2.4 shows the cone diagram of CPTU.

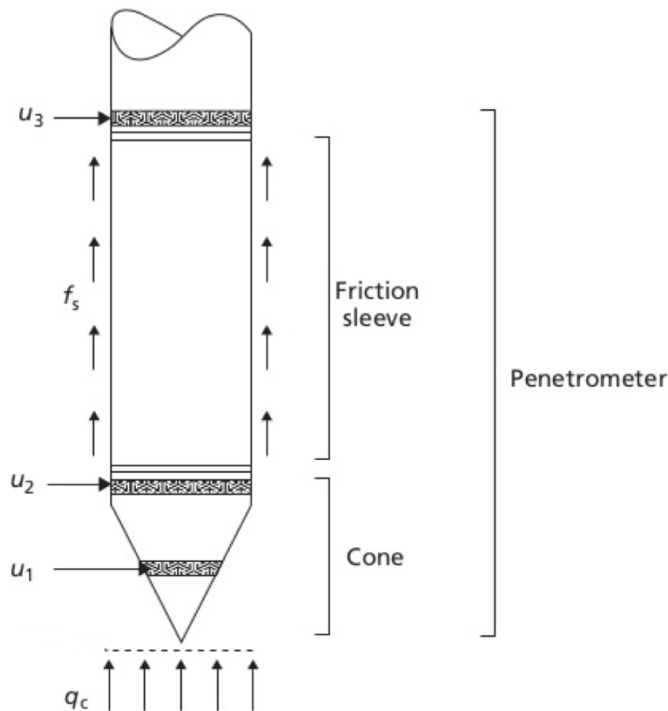


Figure 2.4 Schematic of Piezocone (CPTU) picture taken from (Craig, 2004)

2.2.1 Cone tip resistance

The tip resistance is determined by the force required to push the tip of the cone. Mathematically, its calculated by dividing the force acting on the cone to the area of the cone. Tip resistance is theoretically related to undrained shear strength of saturated cohesive material (Peter Kay Robertson & Campanella, 1986)

Corrected tip resistance

The conical tip is demountable and can be separated from the rest of the probe by a joint. While penetrating, pore pressure will develop and act in this joint. This produce unbalanced

force due to different end areas of the probe components. Therefore, the effect of pore pressure has to be accounted and the corrected tip resistance is calculated by:

$$q_t = q_c + (1 - a)u_2 \quad (2.8)$$

where q_t is corrected cone resistance, q_c is recorded cone resistance, u_2 is total pore pressure in the joint and a is the net area ratio given by; $\frac{A_n}{A_q}$ and depends on probe design. A_n is cross-sectional area of the load cell and A_q is the projected area of the cone.

Chapter 3

Soil variability and Safety

3.1 Soil variability

Soil properties vary spatially. Characterization of this spatial variability is essential for probabilistic interpretation, and a better understanding of the soil parameters. In addition to the variability, measurement errors and modeling assumptions magnify the uncertainties in geotechnical design. Estimation of soil parameters is usually a challenging task due to inherent soil variability. Traditionally, in deterministic stability analysis, high factor of safety is a requirement to cover the uncertainty in characteristic soil parameters. The limitation of this adopted procedure is, it is unable to properly characterize spatial variability and operating with high factor of safety might cause an expensive system. Therefore, it is important that the uncertainties in parameters be adequately quantified and carefully evaluated (Lacasse & Nadim, 1997).

This study describes the probabilistic characterization of soil properties. Probabilistic characterization includes, uncertainties in soil and how the uncertainties in soil properties are distributed, managed and quantified.

3.1.1 Uncertainty

Uncertainties in soil properties are commonly a consequence of inherent soil variability and incomplete knowledge or lack of understanding and insufficient data. Uncertainties associated with geotechnical problem can be divided into two categories, Aleatory uncertainty and Epistemic uncertainty.

Aleatory uncertainty describes inherent natural randomness of natural processes. Inherent variability of soil properties is primarily caused by the natural geologic process in soil formation. Spatial variation of soil parameter within a uniform geological layer is good example. Aleatory uncertainties cannot be eliminated or reduced.

Epistemic uncertainty describes the uncertainty due to lack of knowledge on a variable. It can be caused due to measurement uncertainty, statistical uncertainty because of limited data or model uncertainty. Statistical uncertainties are due to limited information or limited number of observations and can be improved by increasing the number of observations. Measurement error arise due to imperfection of measuring equipment, fault in procedure or random testing effect. This can be minimized by improving measurement accuracy. Model uncertainties develop due to the estimation capability of design model on the real phenomena. Model uncertainty is generally large and can be reduced by improving simulation models (Nadim, 2007). Epistemic uncertainty can be reduced or eliminated.

Uncertain soil properties and model uncertainty are best defined as random variables described by mean trend, standard deviation (or coefficient of variation), correlation function and probability distribution function.

3.1.2 Trend analysis

In chapter 2, it is discussed that, mean value and standard deviation are used to describe variability. But in some cases, two sets of data might have the same mean and standard deviation but reflect different soil conditions as shown in Fig. 3.1. The difference cannot be identified from mean and standard deviation alone. These data can be examined with trend analysis. The trend analysis is conducted by separating the random process into deterministic trend (trend mean) and variability around the trend (Baecher & Christian, 2005).

$$r(z) = t(z) + u(z) \quad (3.1)$$

Where $r(z)$ is the soil property at location z , $t(z)$ is the value of the trend at z , and $u(z)$ is the residual variation.

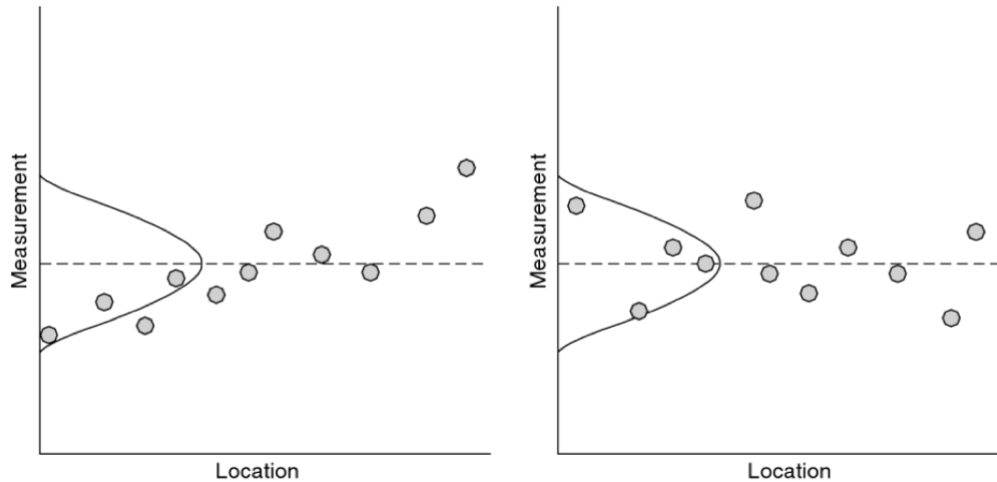


Figure 3.1 Two data having same mean and standard deviation, but different pattern of spatial variation. Picture taken from (Baecher & Christian, 2005)

The residuals are characterized statistically as a random variable. The randomness represents the uncertainty in the difference between the interpolated trend and the actual value of the soil property at the unobserved location. This residual usually described with zero mean, and non-zero variance, $Var[u]$:

$$Var[u] = E[\{r(z) - t(z)\}^2] \quad (3.2)$$

3.1.3 Local average

Characterization of soil parameters are done in a point level by point statistics. The mean value, variance, marginal distribution and so on are defined at point level. However, since soil particles are discontinuous, soil properties are rarely measured at a point. For instance, a volume of soils with in a vicinity of radius about 100 – 200mm are involved in a CPT measurement and CPT cone averages the soil resistance over this volume (Fenton & Griffiths, 2008a). Detail explanation and application of local averaging is described in Section 6.44.

3.2 Random field

Soil properties vary spatially. In addition to errors due to measurement and modeling assumptions, estimations of soil parameters are challenging because of the inherent nature due to geological and pedological soil forming factors. Characterization of this spatial variability is essential for better understanding and can be modeled by using mathematics of random process. Random field provides a method for incorporating spatial variation in engineering and reliability models. It also provides statistical results which can be used to draw inferences from limited field observations (Baecher & Christian, 2005).

Random Field A random field $R(x)$ is defined in \mathbb{R}^n is a function such that for every fixed $x \in \mathbb{R}^n$, $R(x)$ is a random variable in the probability space.

3.2.1 Gaussian random field

Soil properties vary extremely between locations and there is some kind of dependency between neighboring observations depending on the separation distance. The closer the distance, the more the dependence will be. This dependency can be described by joint bivariate distribution, $f_{XY}(x, y)$ meaning, the probability that $X = x$ and $Y = y$ at the same time. The consideration can be extended to infinity but the parameters are difficult to estimate from real data. For simplification, Gaussian Process is assumed. It states, the joint probability density function is a multivariate normally distributed random process (Fenton & Griffiths, 2008b). The great advantage of using Gaussian random field is that the complete distribution can be specified by only mean vector and covariance matrix, and has a form of:

$$f_{X_1 X_2 \dots X_k}(x_1 x_2 \dots x_k) = \frac{1}{(2\pi)^{k/2}} \frac{1}{|C|^{1/2}} \exp \left\{ -\frac{1}{2} (X - \mu)^T C^{-1} (X - \mu) \right\} \quad (3.3)$$

Where, $\mu = E[X]$ is the vector of mean values for X , C is the covariance matrix between the X 's, and given by $C = E[(X - \mu)(X - \mu)^T]$, while the superscript T is for matrix transpose, and $|C|$ is the determinant of the covariance matrix.

For infinite consideration, because of the variation of the mean and the covariance with position, the joint probability function could not be used in practice due to the difficulties to estimate from real data and the mathematical complication. For this reason, the Stationarity assumption will be used to make it more simplified.

Stationarity

A Gaussian random field is said to be stationary if the joint probability function is dependent only on the vector separation among the observations $x_i \dots x_k$ rather than the absolute location. This assumption implies that the mean is $E[R(x_i)] = \mu$ for all x , and the covariance $C[R(x_i), R(x_j)]$ depends only upon vector separation of x_i and x_j not on absolute location. Therefore;

$$C[R(x_i), R(x_j)] = C_R(x_i - x_j) \quad (3.4)$$

3.2.2 Autocorrelation and correlation length

Autocorrelation is a measure that shows the extent at which two values of the same variable fluctuate at distance or time x_i and $x_{i+\tau}$. A measure of dependency between two values of a random variable with in a distance τ , is commonly expressed by correlation coefficient:

$$\rho(x_i, x_j) = \rho(x_i, x_{i+\tau}) = \frac{Cov(x_i, x_j)}{\sigma_{x_i}\sigma_{x_j}} \quad (3.5)$$

Where, the correlation coefficient $\rho(x_i, x_j) = \rho(x_i, x_{i+\tau}) = \rho(x_{i+\tau}, x_i)$ and standard deviations σ_{x_i} and $\sigma_{x_j} = \sigma_x$ for Gaussian stationary random field, while $Cov(x_i, x_j)$ is the covariance between x_i and x_j .

Correlation length, (θ) is one of the measure of variability of random field. It is defined as a distance within which two observations are significantly correlated (the term significantly is defined by more than about 10 % according to Fenton & Griffiths (2008b)).

Relating correlation length with a correlation function, a random process following Markov correlation function with separation distance, τ between two values, has a from:

$$\rho(\tau) = \exp\left\{-2\frac{|\tau|}{\theta}\right\} \quad (3.6)$$

It can be observed that when two observations are close to each other, $\tau \rightarrow 0$, the correlation function will approach to one, $\rho \rightarrow 1$ and in a likely manner, ρ will approach to zero, while the separation distance increases, $\tau \rightarrow \infty$. Contrariwise, for large correlation length, $\theta \rightarrow \infty$, $\rho \rightarrow 1$ and clearly, ρ approaches to zero when θ decreases.

3.2.3 Conditional Gaussian random field

In geotechnical analysis, a number of measurements are made and values of soil property are observed at measured locations. In the process of generating random field, deterministic values are assigned for measured locations, while estimation is made for unobserved locations based on the observed values. Apparently, the soil parameters near the observed locations most likely possess the same or nearly same properties as the observed properties than that of far away. This concept is integrated by conditional random field and described below.

For a Gaussian random field, defined as:

$$R \sim f(r) = N(r; \mu_r, C_r) \quad (3.7)$$

where μ_r is mean, and C_r is covariance matrix with m number of discretization, let $X = (X_1, X_2, \dots, X_n)$ be observed values inside the discretized domain at location (x_1, x_2, \dots, x_n) with covariance matrix between observed points, $C_{x/r}$, then the conditional random field, R given observation X is normally distributed with mean and covariance matrix:

$$\mu_{r/x} = \mu_r + C_r H^T [H C_r H^T + C_{x/r}]^{-1} (X - H \mu_r) \quad (3.8)$$

$$C_{r/x} = C_r - C_r H^T [H C_r H^T + C_{x/r}]^{-1} H \mu_r \quad (3.9)$$

where H is a linear model, defined as a $(n \times m)$ matrix with a value $H(1, x_1) = H(2, x_2) \dots = H(n, x_n) = 1$ and 0 otherwise. The superscript T is standing for matrix transpose.

3.2.4 Generating random field

In reliability analysis, the generated random field realization is considered as an input to the model that simulate the response of the studied structure.

From conditional Gaussian random field, for m number of discretization, the conditional mean, $\mu_{r/x}$ and covariance matrix, $C_{r/x}$ is given by Eqs. 3.8 and 3.9 respectively. By using Cholesky decomposition, $C_{r/x}$ which is a $(m \times m)$ matrix, is decomposed to give a lower A and upper triangle A^T .

$$C_{r/x} = A A^T \quad (3.10)$$

By generating $(m \times 1)$ vector of standard normal distributed random values, $L \sim N(\mu_L = 0, \sigma_L = 1)$, a conditional Gaussian random field realization, R with mean $\mu_{r/x}$, is calculated as:

$$R = \mu_{r/x} + A L \quad (3.11)$$

3.3 Slope stability

3.3.1 Factor of safety

Slope stability analysis is made to check whether a slope is safe or unsafe. The measurer of safety is called factor of safety. Factor of safety can be defined as the ratio between the the average shear strength of the soil, τ_f to the average mobilized shear stress developed

along the potential failure surface, τ_{mob} ($F_s = \frac{\tau_f}{\tau_{mob}}$) and failure is assumed to occur when $F_s < 1$ (Bromhead, 2006). Factor of safety often used as a design criterion. Different countries in the world have different standards for factor of safety to ensure safe design. This values are often based on experience. Table 3.1 shows the factor of safety values required for slopes according to U.S Army Corps of Engineers'. They are intended for application to natural slopes, slopes of embankment dams, other embankment and excavations (Duncan, Wright, & Brandon, 2014).

Table 3.1 Factor of safety criteria from U.S Army Corps of Engineers' slope stability manual

Types of Slopes	Required factor of safety		
	For End of Construction	For Long-Term Steady Seepage	For Rapid Draw-down
Slopes of dams, levees and dikes, and other embankment and excavation slopes	1.3	1.5	1.0 - 1.2

There are different types of numerical techniques used to analyze the stability of slope.

Limit equilibrium method investigates the stability of a soil mass tending to slide down transitionally or rotationally by assuming potential slip surface (Army, 2003).

Finite element method (FEM) is a numerical technique used to find the approximate solution to partial differential equations. In slope stability, the large slope divided into smaller elements and the analysis at each element assembled to represent the large slope. The main advantage of FEM over limit equilibrium is, shape and location of failure surface is not assumed and failure mechanism develop freely by detecting the weakest zone. Different types of soil models can be computed using different failure criteria with complex slope configuration. In this thesis FEM method is used with computer programing, PLAXIS 2D.

3.3.2 Probabilistic slope stability method

The main limitation of factor of safety is, it does not describe how safe a slope is and limited on providing the likelihood of the design failure. Uncertainties in the input parameters also affect the failure likelihood. This is best handled with probabilistic analysis. Probabilistic analysis method, in general, provides a tool to quantify the possible risk associated with failure and assesses the reliability of a slope. To handle uncertainty, input parameters are treated as random variables described by their corresponding distribution type, measure of tendency (mean), and variability (standard deviation).

Single random variable approach (SRV) is a probabilistic analysis method so that the input mechanism is based on distribution type, mean value and standard deviation of the parameter. A single random value is assigned for the entire slope or for the corresponding one layer in the case where slope is made up of different layers. This means, the value of the parameter does not change with in a layer (Fenton & Griffiths, 2008d).

Random finite element method (RFEM) is a combined effect of random field with a finite element method. It follows the same method as SRV on assigning random values for parameters, but one value is assigned for one discretized element instead of one layer.

These input parameters directly incorporated to the analysis model using sampling techniques. Many commercial software programs are available to carry out such kind of computations automatically.

3.3.3 Monte Carlo sampling technique

In probabilistic slope stability analysis, the shear strength input parameters such as undrained shear strength for clay and friction angle for sand, are not deterministic and treated as random variable. The values of these parameters can be distributed about their means in a manner which can be described by one of the continuous distribution functions. This information can not be used directly in the analysis. Sampling methods incorporate this given information and provide an input value for the analysis (FEM). One of the simplest sampling method is Monte Carlo method and used in this study.

Monte Carlo (MC) simulation is a numerical simulation that generates random or pseudo random numbers based on the given probability distribution. All numbers within the distribution have the same chance of probability for being selected. The generated samples then can be used in a calculation and for each sample the corresponding output is collected. From the collected output, distribution of factor of safety and failure probability can be computed. The Monte Carlo simulation is well suited for slope stability analysis where several random parameters exist or if the slope is a combination of different layers while each layer is represented with random variable.

Chapter 4

Description of Rissa Area

4.1 Rissa landslide

Rissa is a municipality in Sør-Trøndelag county, Norway. It is part of the Fosen region. In April 1978, Rissa was home to a quick clay landslide which encompassed an area of 330,000 square meters and a flow of 6,000,000 cubic meters of clay from the Årnset area on the shore into Botn, causing a miniature tsunami on the north shore in Leira (Gregersen, 1981). Figure 4.1 shows a picture taken during the landslide (picture taken from Google Maps). A lot of researches have been done in the area to study the event.



Figure 4.1 Rissa landslide occurred on 29 April, 1978

4.2 Background information

The Norwegian Public Roads Administration (NPRA) was planning to build a new road, RV 717 between Sund and Bradden in Rissa, located on the peninsula Fosen, northwest of Trondheim in Rogaland county as shown in Figure 4.2.



Figure 4.2 Aerial Photography map of Rissa showing the planned road alignment (Google Maps)

This coastal area is covered with marine deposits. The planning works started in 2009 but were halted due to the geotechnical challenges of the project and the marginal safety factor of the area. There is a gentle slope between Rein Church and Botn lake consisting of sensitive clay. The slope is located on the other side of the lake where Rissa landslide took place. The area has been studied previously with several laboratory experiments, total soundings, CPTU and R CPTU (resistivity), block samples. Block samples were taken by NTNU, supported by the Public Roads Administration. Field and laboratory test results are compiled and presented by Kornbrekke (2012).

The area around Lake Botn is covered by a thick layer of sea deposits. These sea deposits sit directly on the rock surface. The other dominating soil type is, the marine deposits that cover the western parts of the area. The marine deposits are formed when the glacial were retreating approximately 12,500 years ago. The glacial had melted in the Rissa area around 9000 years ago. After that the land heaved around 158 m over the former coastal line. The land heave has exposed the marine clay for fresh water that have washed out the salt and lowered strength. This have lead to the formation of quick clay in some parts of the area (Kornbrekke, 2012).

4.3 Ground investigations

Ground investigations have been performed several times. Norwegian Geotechnical Institute, NGI has made the first ground investigations in 2007 in connection with the first detail planning of the project. Additional investigations were made in 2009.

The NGI ground investigations showed the presence of quick clay in the area. In 2011, NGI performed a slope stability analysis based on data from their own investigations and the investigations that NPRA have been made from 1974 to 2009. It is found to be that the areas around Reinsalléen and Åsen are the most susceptible to failure. The road construction was planned to pass by Reins church but halted due to the low factor of safety which failed to fulfill the regulations.

Geological survey of Norway, NGU in cooperation with a master student from Norwegian University of Science and Technology, NTNU made electrical resistivity measurement during 2009 to 2010. In 2011 and 2012, NGU continued the geophysical investigations and made a seismic refraction measurement around Lake Botn and Rein church. In 2011 Geo-Vest Haugland and Multiconsult performed extensive ground investigations.

In this thesis, a specific slope, section 3-3 profile C is chosen and all the available data are used from Statens Vegvesen (NPRA). The geometry of the slope, section profile, soil stratification and CPT profile points are shown in Figure 4.3.

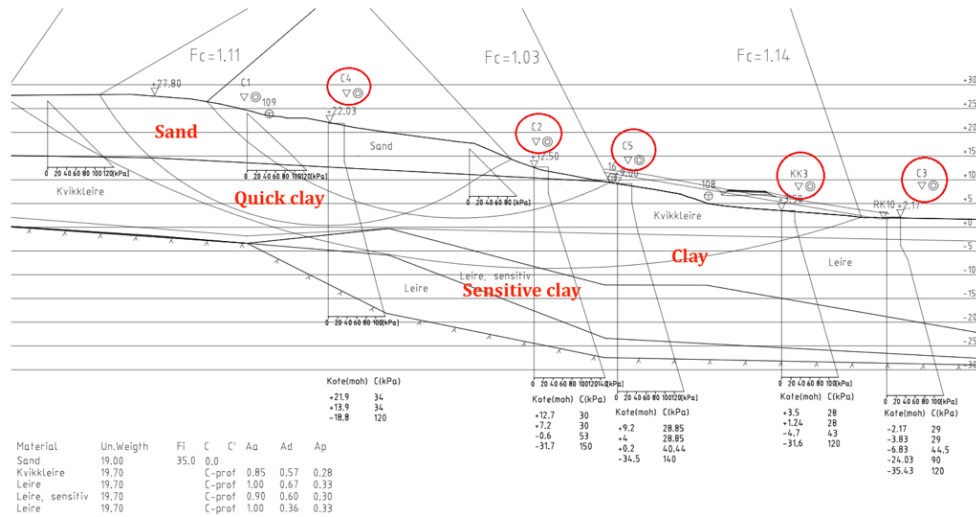


Figure 4.3 Geometry, soil layering and CPT profile points of Rissa slope, section 3-3 profile C

The horizontal length of the slope is around 210m. The highest elevation, left top, is +28m and the lowest, right bottom is -28m. The slope is resting on bedrock. CPTU investigation has been made on different positions within the slope. C4, C2, C5, KK3, and C5 are CPTU profiles as shown in Figure 4.3. The data from the CPT measurements are used for probabilistic interpretation of soil parameters and the methods are described in chapter 5. summary of the test results with soil layering depth, and ground water level depth are presented in Table 4.1.

Table 4.1 Soil layering and ground water depth of CPT profiles

	Layer depth				
	C4	C2	C5	KK3	C3
GWL	1.27m	2.35m	1.85m	2.00m	2.00m
Sand	0 - 8m	0 - 2m			
Quick Clay	8 - 23m	2 - 11m	0 - 11m	0 - 6.5m	0 - 4.5m
Clay	below 23m	11 - 18m	11 - 21m	6.5 - 18.5m	4.5 - 15m
Sensitive clay		below 18m	below 21m	below 18.5m	below 15m

Chapter 5

Probabilistic interpretation of soil parameters from CPT

5.1 Estimation of correlation length

All possible soil parameters should be estimated to represent a particular soil variability with more certainty. One of the interesting parameters in representing spatial variability is correlation length. Maximum likelihood estimation (MLE) method is one of the many different ways used to estimate the correlation length from CPT data.

5.1.1 Maximum likelihood estimation

Maximum likelihood method is a process and procedure of estimating values of one or more parameters for a given statistical model data which makes the known likelihood distribution a maximum (Harris & Stöcker, 1998). It is more efficient when the data are normally distributed or somehow have been transformed from their actual state to approximate normal distribution (Fenton & Griffiths, 2008a).

The likelihood, L of observing a sequence of normally distributed observations $X = \{x_1, x_2, \dots, x_n\}$ given the distribution parameters, mean μ_x , variance σ_x^2 , and correlation length, θ is:

$$L(x/\mu_x, \sigma_x^2, \theta) = \frac{1}{(2\pi\sigma_x^2)^{n/2} |\rho|^{1/2}} \exp \left\{ -\frac{(x - \mu)^T \rho^{-1} (x - \mu)}{2\sigma_x^2} \right\} \quad (5.1)$$

Where, ρ is a correlation function given as a function of the correlation length, θ . In this study a Markov correlation function is used and described in Eq. 3.6. $|\rho|$ and ρ^{-1} are the determinant and inverse of ρ respectively. μ is a vector of means corresponding to each observed location. $(x - \mu)^T$ is vector transpose for $(x - \mu)$.

Since the likelihood function is nonnegative, maximizing $L(x/\mu_x, \sigma_x^2, \theta)$ is equivalent to maximizing its logarithm, $\mathcal{L}(x/\mu_x, \sigma_x^2, \theta)$, which ignores constants. After making a partial derivation of the likelihood function with each unknown parameters, $\mu_x, \sigma_x^2, \theta$, the logarithm likelihood function, \mathcal{L} is calculated as:

$$\mathcal{L} = -\frac{n}{2}(\ln \sigma^2 + \ln|\rho|) \quad (5.2)$$

From Rissa CPT measurements, for the observed corrected cone tip resistance q_t , which is log normally distributed (determined on the previous project) and the equivalent normally distributed, $Y = \ln q_t$, with depth dependent mean trend, $\mu_{\ln q_t}$ and depth, z defined by a

matrix F as $F = \begin{pmatrix} 1 & z_1 \\ \vdots & \vdots \\ 1 & z_n \end{pmatrix}$, the regression problem,

$$F \mu_{\ln q_t} = Y \quad (5.3)$$

has the generalized least square solution:

$$\mu_{\ln q_t} = (F^T \rho^{-1} F)^{-1} F^T \rho^{-1} Y \quad (5.4)$$

and the variance estimate:

$$\sigma_{\ln q_t}^2 = \frac{1}{n} (Y - F \mu_{\ln q_t})^T \rho^{-1} (Y - F \mu_{\ln q_t}) \quad (5.5)$$

The matrix ρ , $\mu_{\ln q_t}$ and $\sigma_{\ln q_t}^2$ are dependent on θ . The optimal choice θ is then defined as the maximum likelihood estimator, the maximizer of:

$$\mathcal{L} = -\frac{n}{2}(\ln \sigma_{lnqt}^2 + \ln |\rho|) \quad (5.6)$$

The solution for the maximum likelihood estimator, \mathcal{L} is determined with iteration process by guessing value for θ at first. Probable range of θ is selected and the corresponding \mathcal{L} values are computed by the equations given above. The most likely value of θ that gives the maximum value of \mathcal{L} is then identified by making θ verses \mathcal{L} plot as shown in Fig. 5.1.

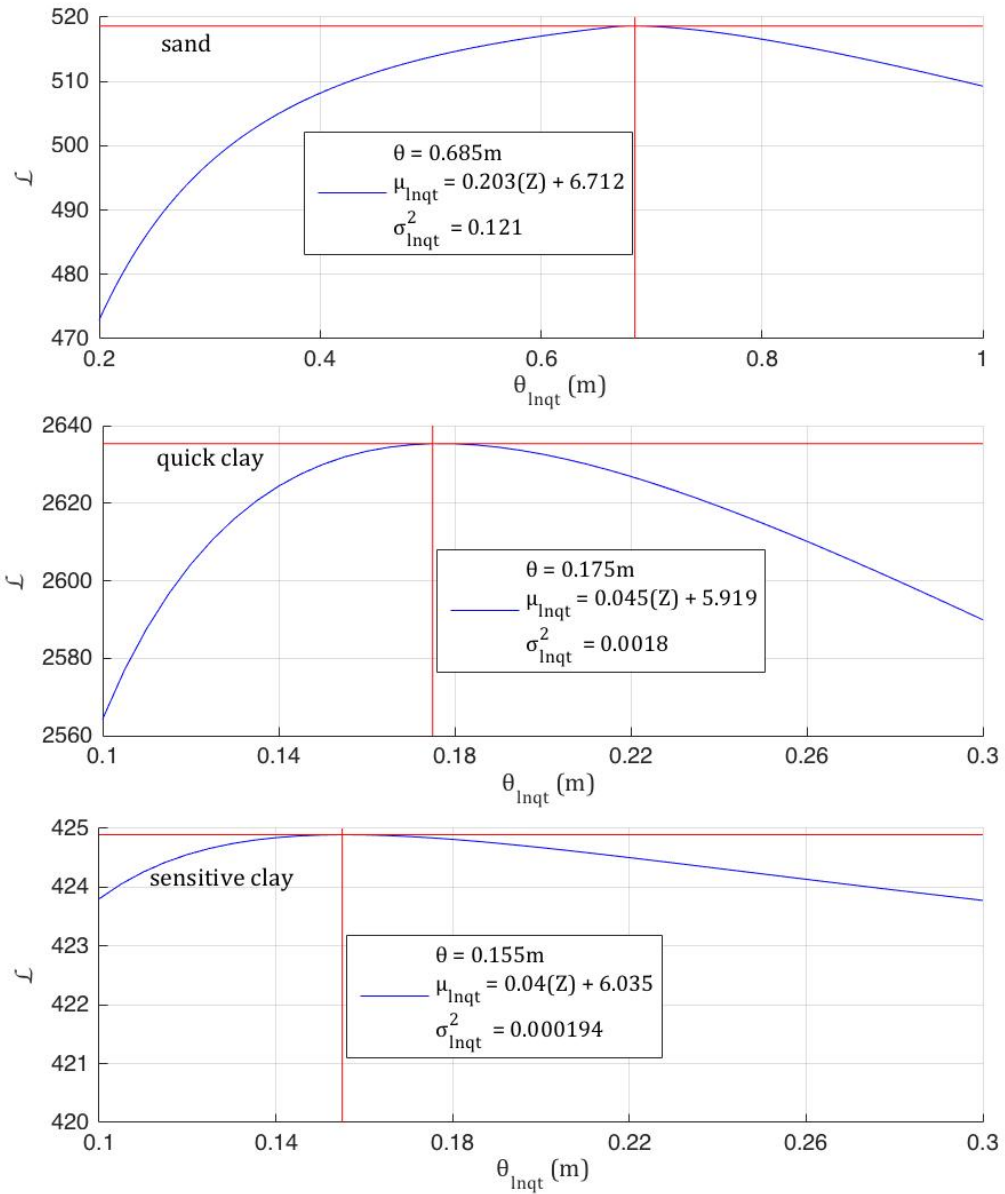


Figure 5.1 Log-likelihood function for a range of correlation lengths, θ_{lnqt} for C4

As shown in the geometry of Rissa slope, Fig. 4.3, different types of soil layers are identified. Each layer is assumed to be statistically homogeneous so that the correlation length holds same only within a certain layer and vary when enters to another layer. This is shown in Fig. 5.1, for a single CPT profile C4, different layers have different correlation length values.

The computed results for all other profiles are summarized in Table 5.1.

Table 5.1 Maximum likelihood estimation result for $\theta_{\ln q_t}$, $\mu_{\ln q_t}$, and $\sigma_{\ln q_t}^2$ for all profiles

<i>Profile</i>	<i>Soil Type</i>	$\theta_{\ln q_t} (m)$	$\mu_{\ln q_t}$	$\sigma_{\ln q_t}^2$
C4	<i>Sand</i>	0.685	0.203 (Z) + 6.712	0.121
	<i>Quick Clay</i>	0.175	0.045 (Z) + 5.919	0.0018
	<i>Sensitive Clay</i>	0.155	0.040 (Z) + 6.035	0.000194
C2	<i>Quick Clay</i>	0.34	0.074 (Z) + 5.699	0.0028
	<i>Clay</i>	0.4	0.037 (Z) + 6.197	0.0027
	<i>Sensitive Clay</i>	0.205	0.029 (Z) + 6.294	0.0024
C5	<i>Quick Clay</i>	0.32	0.071 (Z) + 5.634	0.0018
	<i>Clay</i>	0.3	0.054 (Z) + 5.875	0.0019
	<i>Sensitive Clay</i>	0.51	0.054 (Z) + 5.863	0.0027
KK3	<i>Quick Clay</i>	0.25	0.145 (Z) + 5.019	0.015
	<i>Clay</i>	0.49	0.061 (Z) + 5.674	0.0039
	<i>Sensitive Clay</i>	0.29	0.039 (Z) + 6.122	0.003
C3	<i>Quick Clay</i>	0.45	0.012 (Z) + 5.894	0.003
	<i>Clay</i>	0.245	0.062 (Z) + 5.689	0.0013
	<i>Sensitive Clay</i>	0.21	0.039 (Z) + 6.009	0.001

5.2 Probabilistic interpretation of shear strength of soil

In slope stability analysis the main inputs are shear strength parameters of soil. That is undrained shear strength for clay soil, and friction angle for sand. These parameters can be quantitatively derived from the available CPT data. If someone wants to extend the stability analysis further to a probabilistic one, strength parameters are needed to be described probabilistically, and all the possible uncertainties in the derivation process should be quantified and accounted. The methods to drive probabilistic shear strength parameters of soil from CPT data which accounted for uncertainty is detailed in here.

5.2.1 Undrained shear strength

There are several methods available to estimate undrained shear strength, S_u of clays of different type. One of the earliest application of CPT in soil exploration is determining the undrained shear strength of clays (Schmertmann, 1975). Due to the common interpretation of S_u from CPT measurements, S_u is linked with significant uncertainties.

In geotechnical practice, classical interpretation of S_u by corrected cone tip resistance, q_t from CPT measurements in clays is given by (Lunne, Robertson, & Powell, 1997):

$$S_u = \frac{q_t - \sigma_{vo}}{N_{kt}} \quad (5.7)$$

Where σ_{vo} is the insitu total overburden stress and N_{kt} is the empirical cone penetration resistance factor. All the parameters used to interpret S_u are subjected to uncertainty. The uncertainties in q_t are a result of inherent soil variability and measurement error. Soil variability is caused primarily by natural geological process involved during soil formation, while measurement error arises from equipment, procedural operator and random testing effect (Phoon & Kulhawy, 1999). The uncertainty from soil variability is considered to be statistical error and appointed in mean trend and variance estimation of q_t . q_t is lognormally distributed and the normal depth dependent mean trend, μ_{lnq_t} and variance $\sigma_{lnq_t}^2$ are

directly determined by maximum likelihood estimation method, after computing the correlation length for each soil layers as presented in Table 5.1.

The measurement error, ϵ_q is considered as lognormally distributed with a unit mean and *CoV* to be 10%. The *CoV* value is selected based on the CPT equipment type as stated by Phoon and Kulhawy (Phoon & Kulhawy, 1999).

σ_{vo} can also be influenced by soil variability and measurement error. In this study a deterministic stress state is assigned for σ_{vo} that depends on the unvaried soil unit weight, γ_s for each soil type due to relatively low variability (Lacasse & Nadim, 1997), stable ground water level and soil depth.

N_{kt} is obtained by empirical correlation and there is no constant N_{kt} value that can represent each clay types (P. K. Robertson & Campanella, 1983b). It is complicated to define a single soil property that governs N_{kt} because there are more factors affecting the values of N_{kt} like clay sensitivity, plasticity index of the clays tested, and the type of cone used.

For Rissa area, the N_{kt} values are presented as a deterministic value with possible plus or minus range. It has been stated in the report that the values are determined from a combined impact of the variables B_q, St, OCR, Ip . These values vary from one CPT profile to another and through out depth within a single profile.

To create a probabilistic link between undrained shear strength and the cone factor, in this report, N_{kt} is assumed to be lognormally distributed with a mean same as the deterministic value given in the report. Coefficient of variation, $CoV = 30\%$ is used as reported by Kulhawy and Carter, based on the the types of tests (F. Kulhawy & Carter, 1992) to include the inherent bias (Fell, MacGregor, Stapledon, & Bell, 2005).

All the input parameters values and the quantified uncertainties used for probabilistically interpreting undrained shear strength of clay of profile C4 are summarized and presented in Table 5.2. The normal mean trend and variance of $\ln qt$ is taken from Table 5.1.

Table 5.2 Input values of parameters used for probabilistic interpretation of S_u for clay layers of profile C4

<i>C4 Profile</i>		
<i>Parameters</i>	<i>Quick Clay</i>	<i>Sensitive Clay</i>
$\mu_{\ln q_t}$	$0.045 (Z) + 5.919$	$0.040 (Z) + 6.035$
$\sigma_{\ln q_t}^2$	0.0018	0.000194
μ_{ϵ_q}	1	1
CoV_{ϵ}	0.1	0.1
$\mu_{N_{kt} 1}$		9
$\mu_{N_{kt} 2}$		6
$CoV_{N_{kt}}$		0.3

$\mu_{N_{kt} 1}$ and $\mu_{N_{kt} 2}$ are mean cone factor values for depth less than 16m and greater than 16m respectively as stated in the Rissa Slope Report

The probabilistic derivation of S_u from q_t including CPT measurement error, ϵ_q is then given by:

$$S_u = \frac{\epsilon_q q_t - \sigma_{vo}}{N_{kt}} \quad (5.8)$$

The logarithmic transformation of Eq. 5.8 gives the parameter $\ln S_u$, given by:

$$\ln S_u = \ln(\epsilon_q q_t - \sigma_{vo}) - \ln N_{kt} \quad (5.9)$$

The product of two lognormal random variables (ϵ_q and q_t) is lognormally distributed with mean $\mu_{\epsilon_q q_t}$ and standard deviation $\sigma_{\epsilon_q q_t}$. The distribution parameters are calculated by utilizing the relation to the normal distribution:

$$\ln(\epsilon_q q_t) = \ln \epsilon_q + \ln q_t \quad (5.10)$$

The sum of normally distributed random variable is normally distributed with mean and variance:

$$\mu_{\ln(\epsilon_q q_t)} = \mu_{\ln \epsilon_q} + \mu_{\ln q_t}; \quad \sigma_{\ln(\epsilon_q q_t)}^2 = \sigma_{\ln \epsilon_q}^2 + \sigma_{\ln q_t}^2 \quad (5.11)$$

Where, $\mu_{\ln q_t}$ and $\sigma_{\ln q_t}^2$ are the mean and variance of $\ln q_t$ as computed by maximum likelihood estimation method and presented in Table 5.1. $\mu_{\ln \epsilon_q}$ and $\sigma_{\ln \epsilon_q}^2$ are the mean and variance of $\ln \epsilon_q$, calculated as:

$$\sigma_{\ln \epsilon_q}^2 = \ln \left(1 + \frac{\sigma_{\epsilon_q}^2}{\mu_{\epsilon_q}^2} \right); \quad \mu_{\ln \epsilon_q} = \ln \mu_{\epsilon_q} - \frac{1}{2} \sigma_{\ln \epsilon_q}^2 \quad (5.12)$$

The product $\epsilon_q q_t$ is lognormally distributed with mean and standard deviation:

$$\mu_{\epsilon_q q_t} = \exp \left(\mu_{\ln(\epsilon_q q_t)} + \frac{1}{2} \sigma_{\ln(\epsilon_q q_t)}^2 \right) \quad (5.13)$$

$$\sigma_{\epsilon_q q_t} = \mu_{\epsilon_q q_t} \sqrt{\exp \left(\sigma_{\ln(\epsilon_q q_t)}^2 \right) - 1} \quad (5.14)$$

σ_{vo} being deterministic, it only affect the mean value of $\epsilon_q q_t$ keeping the standard deviation unchanged. Then, $(\epsilon_q q_t - \sigma_{vo})$ is lognormally distributed with mean and standard deviation:

$$\mu_{(\epsilon_q q_t - \sigma_{vo})} = \mu_{\epsilon_q q_t} - \sigma_{vo}; \quad \sigma_{(\epsilon_q q_t - \sigma_{vo})} = \sigma_{\epsilon_q q_t} \quad (5.15)$$

Since all the terms on Eq. 5.9 are normally distributed, the mean and variance of a normally distributed $\ln S_u$ is calculated by:

$$\mu_{\ln S_u} = \mu_{\ln(\epsilon_q q_t - \sigma_{vo})} - \mu_{\ln N_{kt}}; \quad \sigma_{\ln S_u}^2 = \sigma_{\ln(\epsilon_q q_t - \sigma_{vo})}^2 + \sigma_{\ln N_{kt}}^2 \quad (5.16)$$

where $\mu_{\ln(\epsilon_q q_t - \sigma_{vo})}$ and $\sigma_{\ln(\epsilon_q q_t - \sigma_{vo})}$ are parameters of $\ln(\epsilon_q q_t - \sigma_{vo})$, while $\mu_{\ln N_{kt}}$ and $\sigma_{\ln N_{kt}}$ are parameters of $\ln N_{kt}$ and calculated as:

$$\sigma_{\ln(\epsilon_q q_t - \sigma_{vo})} = \sqrt{\ln\left(1 + \frac{\sigma_{(\epsilon_q q_t - \sigma_{vo})}^2}{\mu_{(\epsilon_q q_t - \sigma_{vo})}^2}\right)} \quad (5.17)$$

$$\mu_{\ln(\epsilon_q q_t - \sigma_{vo})} = \ln \mu_{\ln(\epsilon_q q_t - \sigma_{vo})} - \frac{1}{2} \sigma_{\ln(\epsilon_q q_t - \sigma_{vo})}^2 \quad (5.18)$$

$$\sigma_{\ln N_{kt}} = \sqrt{\ln\left(1 + \frac{\sigma_{N_{kt}}^2}{\mu_{N_{kt}}^2}\right)}; \quad \mu_{\ln N_{kt}} = \ln \mu_{N_{kt}} - \frac{1}{2} \sigma_{\ln N_{kt}}^2 \quad (5.19)$$

Knowing that $\ln S_u$ is normally distributed, S_u is lognormally distributed with the mean and standard deviation:

$$\mu_{S_u} = \exp\left(\mu_{\ln S_u} + \frac{1}{2} \sigma_{\ln S_u}^2\right); \quad \sigma_{S_u} = \mu_{S_u} \sqrt{\exp(\sigma_{\ln S_u}^2) - 1} \quad (5.20)$$

The correlation length in section 5.1.1 is computed from the underlying normal distribution, $\ln q_t$. However, $\theta_{\ln q_t}$ is assumed to be not much different from the correlation length in real space. Therefore, $\theta_{\ln q_t} = \theta_{q_t}$ (Fenton & Griffiths, 2008d). It is also assumed that the correlation length will remain same for all the parameters though out the derivation process so that the transformation only affects the mean and variance, while the the auto-correlation properties remain unchanged, $\theta_{S_u} = \theta_{q_t} = \theta_{\ln q_t}$.

Following all the procedures mentioned above, the calculated mean value of S_u and the 90% interval estimates of S_u (90% confidence interval (CI) with upper and lower limit) are presented for profile C4 in the Fig. 5.2. The depth, Z starts approximately from 8m

because of the presence of sand layer on top for this specific profile which will be dealt on the next section.

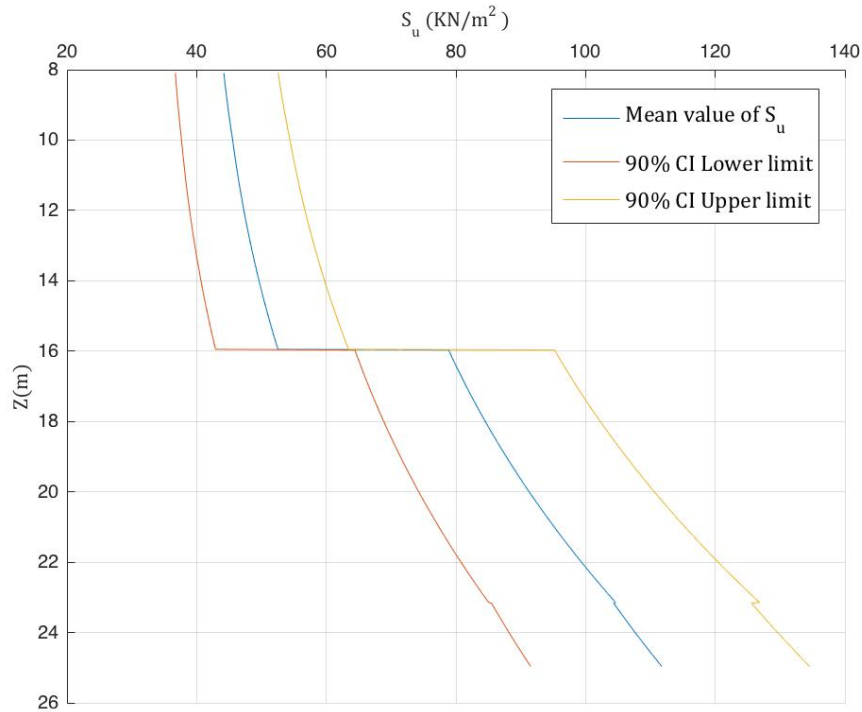


Figure 5.2 Mean value of S_u with 90% confidence interval for profile C4 clay layers

5.2.2 Friction angle

There are theories and empirical correlations for the interpretation of friction angle of sand from cone resistance based on bearing capacity theory (Durgunoglu & Mitchell, 1973), (Senneset & Janbu, 1985). Work by Vesic (Vesic, 1963) has shown the influence of the soil compressibility on cone resistance, and the existence of non unique relationship between friction angle for sand and cone resistance. This is mainly due to the compressibility parameters will also control penetration resistance beside the shear strength of the sand. Al-Awkati (1975) in his work shows that shear strength has significantly more influence on cone resistance than compressibility due to the fact that variation in compressibility is low and can be ignored when compared to the possible variation of shear strength (Al-

Awkati, 1975). Thus bearing capacity theories with a neglected influence of compressibility has been used and produce reasonable estimates of friction angle (P. K. Robertson & Campanella, 1983a). Accordingly, the point resistance can be approximated by:

$$q_t = (N_q - 1)\sigma'_{vo} \quad (5.21)$$

Where, σ'_{vo} is the effective vertical stress at the depth of penetration and N_q is bearing capacity ratio. For a firm sand soil (plasticity angle, $\beta = 0$), N_q is calculated using the formula:

$$N_q = \tan^2\left(\frac{\pi}{4} + \frac{\varphi}{2}\right) \exp(\pi \tan \varphi) \quad (5.22)$$

Where, φ is friction angle. The uncertainties in corrected tip resistance, q_t are discussed in section 5.2.1. Even though σ'_{vo} is subjected to varies uncertainties, in this study a deterministic effective stress state that depends on the unvaried soil unit weight γ_s and fixed ground water table is used.

Combining Eq. 5.21 and Eq. 5.22, it can be realized that q_t is directly related to both vertical stress, σ'_{vo} and friction angle, φ for $0 < \varphi < 90^\circ$. Therefore, φ is positively correlated to the ratio q_t/σ'_{vo} . Its possible to get the value for φ by solving Eq. 5.21 and Eq. 5.22 simultaneously. But, the derivation of an expression for φ as a function of q_t and σ'_{vo} is a challenging task. However, once all the values of φ is computed for each values of q_t and σ'_{vo} , φ can be approximated well with a relatively simple log-regression model for values of q_t/σ'_{vo} as shown in Fig 5.3.

The approximated regression model has a form:

$$\varphi = 7.55 \ln\left(\frac{q_t}{\sigma'_{vo}}\right) + 8.67 + \epsilon_R \quad (5.23)$$

Where, ϵ_R is normally distributed regression model error with zero mean and standard deviation equal to the root mean square error of the regression model, $\sigma_{\epsilon_R} = 0.19^\circ$.

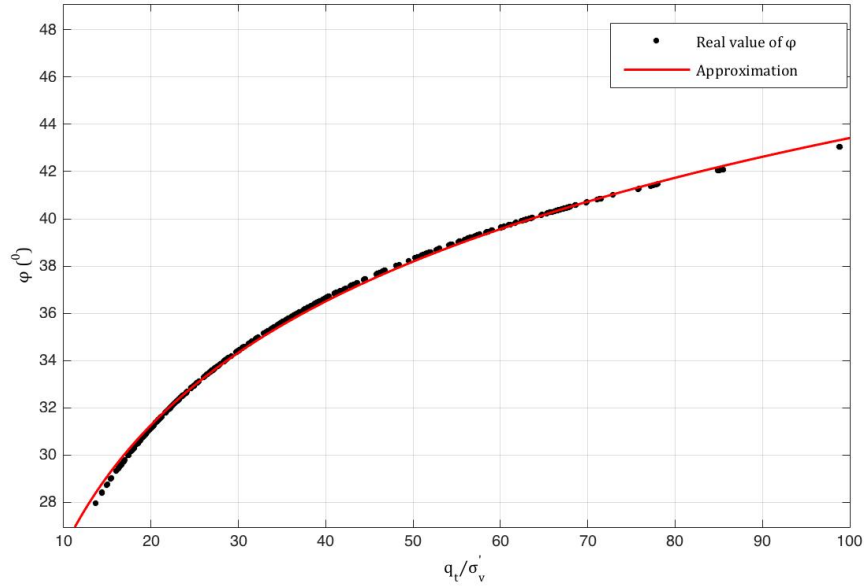


Figure 5.3 Computed values of φ using Eq. 5.21 and Eq. 5.22 with the fitted regression model having a form as Eq.5.23

Including the measurement error ϵ_q for q_t , which is lognormal distributed with $\mu_{\epsilon_q} = 0$ and $\sigma_{\epsilon_q} = 0.1$ as discussed in section 5.2.1, and accounting for the transformation error, ϵ_T , the transformed model will become:

$$\varphi = 7.55 \ln \left(\frac{\epsilon_q q_t}{\sigma'_{v0}} \right) + 8.67 + \epsilon_R + \epsilon_T \quad (5.24)$$

ϵ_T is normally distributed random variable with mean, $\mu_{\epsilon_T} = 0$ and standard deviation is to be obtained by calibrating the transformation in Eq. 5.23 from the observed values. Kulhawy and Mayne obtained an estimate of $\sigma_{\epsilon_T} = 2.8^\circ$ after employing a log-regression model for sand (F. H. Kulhawy & Mayne, 1990). Incorporating all random variables, the normally distributed φ can be described with parameters:

$$\mu_\varphi = 7.55 \left(\mu_{\ln \epsilon_q} + \mu_{\ln q_t} - \ln \sigma'_{v0} \right) + 8.67 \quad (5.25)$$

$$\sigma_\varphi^2 = 7.55^2 \left(\sigma_{\ln \epsilon_q}^2 + \sigma_{\ln q_t}^2 \right) + \sigma_{\epsilon_R}^2 + \sigma_{\epsilon_T}^2 \quad (5.26)$$

Where, $\mu_{\ln q_t}$ and $\sigma_{\ln q_t}^2$ are the mean and variance of $\ln q_t$ computed by MLE method and presented in Table 5.1. $\mu_{\ln \epsilon_q}$ and $\sigma_{\ln \epsilon_q}^2$ are the mean and variance of normally distributed $\ln \epsilon_q$, derived using Eq. 5.12.

All the input parameters values and the quantified uncertainties used for probabilistically interpreting friction angle of sand layer of profile C4 are summarized and presented in Table 5.4.

Table 5.3 Input parameters' values used for probabilistic interpretation of φ of sand layer of profile C4

<i>C4 Profile</i>	
<i>Parameters</i>	<i>Sand</i>
$\mu_{\ln q_t}$	$0.203 (Z) + 6.712$
$\sigma_{\ln q_t}^2$	0.121
μ_{ϵ_q}	1
σ_{ϵ_q}	0.1
μ_{ϵ_R}	0
σ_{ϵ_R}	0.19^0
μ_{ϵ_T}	0
σ_{ϵ_T}	2.8^0

The correlation length in section 5.1.1 is computed from the underlying normal distribution, $\ln q_t$. However, $\theta_{\ln q_t}$ is assumed to be not much different from the correlation length in real space. Therefore, $\theta_{\ln q_t} = \theta_{q_t}$ (Fenton & Griffiths, 2008d). It is also assumed that the correlation length will remain same for all the parameters though out the derivation process so that the transformation only affects the mean and variance, while the the auto-correlation properties remain unchanged, $\theta_\varphi = \theta_{q_t} = \theta_{\ln q_t}$.

Following all the procedures mentioned above, the calculated mean value of φ and the 90% interval estimates (90% confidence interval (CI) with upper and lower limit) of φ are presented in the Fig. 5.4.

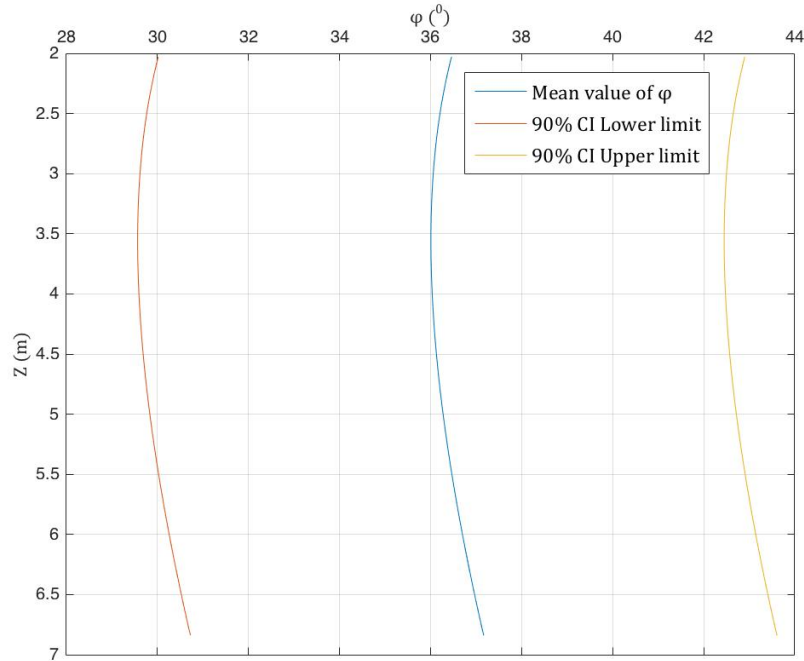


Figure 5.4 Mean value of φ with 90% confidence interval for profile C4, sand layer

Fig. 5.4 shows curved shape plot for mean friction angle with depth. The reason for this is clearly described in Eq. 5.25. Both $\mu_{\ln q_t}$ and vertical effective stress, σ'_{vo} are linear with depth and all the other parameters in the equation are constants and do not affect the shape of the graph. However, the logarithm of σ'_{vo} will follow a logarithmic curve and the numerical subtraction, $\mu_{\ln q_t} - \ln \sigma'_{vo}$ will result a convex type curve bulged outwards as illustrated in Fig. 5.4.

Chapter 6

Results

6.1 Slope stability analysis

The main purpose of this paper is to introduce and implement advanced probabilistic slope stability analysis method, that is conditional random finite element method (CRFEM) approach on Rissa slope. Other non-probabilistic and simple probabilistic slope stability analysis methods are also implemented and presented in this chapter briefly. This is mainly to demonstrate the effect of the analysis method transition from deterministic stability approach to simple probabilistic one and again to more complex slope stability, CRFEM approach. Initially, the slope is investigated using traditional approach with a constant, one deterministic value for each soil layer. Simple probabilistic concept is then implemented with random variable technique governed by mean value and standard deviation of the parameters. Finally, a number of different simulations have been made using CRFEM approach by varying the values of unobserved parameters (unobserved standard deviation and horizontal correlation length) and lastly, local averaging concept is implemented and the effect on CRFEM is assessed.

6.2 Deterministic slope stability method

Traditionally, a fixed soil parameter value is assigned for each soil layer. There is no variation in properties within a layer. The shear strength parameters are computed directly from CPT using q_t without incorporating any uncertainty. The computed results from all CPT profiles within a specific soil layer are collected and the one average value is set to

be the shear strength of the corresponding layer. The PLAXIS 2D input geometry of the slope with layer stratification is shown in Fig. 6.1.

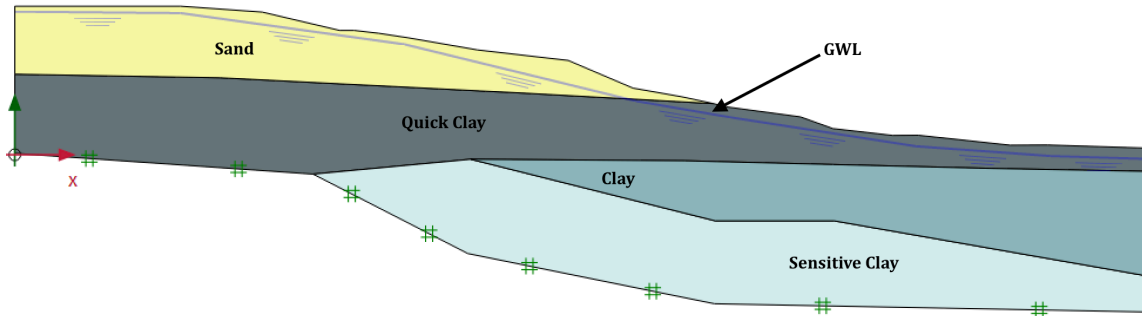


Figure 6.1 Plaxis 2D input Geometry of Rissa Slope

The computed deterministic shear strength values are summarized in the table below.

Table 6.1 Plaxis 2D deterministic input parameters

Layer	γ_s (KN/m ³) ¹	S_u (KN/m ²)	φ (^o)	a (KN/m ²)
Sand	19.0		38.94	10
Quick Clay	19.7	42.80		
Clay	19.7	56.53		
Sensitive				
Clay	19.7	94.50		

The superscript¹ is to indicate that the values are directly taken from Rissa Slope Report

The likely failure mechanism in terms of deviatoric strain is presented in Fig.6.2. The computed factor of safety is equal to 1.022. It is close to the value described in Rissa Slope Report which is 1.03. This can be taken as a grant for the precision of the slope geometry and the resemblance of the analyses method used with the one described here.

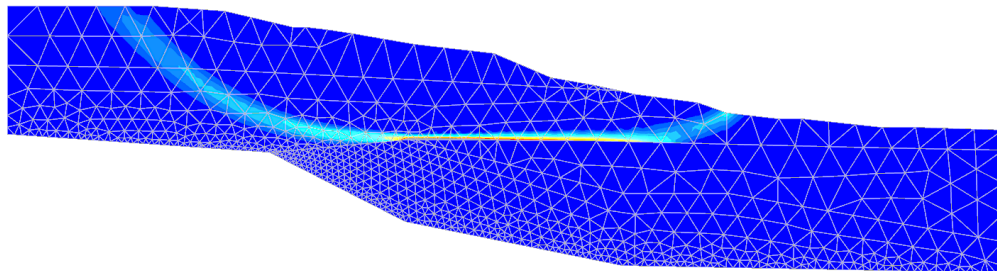


Figure 6.2 Failure mechanism of the slope in terms of deviatoric strain

6.3 Single Random Variable method

This method is similar to the deterministic approach in a way that only a single parameter value is assigned for each layer. But the assigning process is governed by generating random values based on the distribution type, mean value and standard deviation of parameters. In this probabilistic method, assigning same uniform shear strength value for each layer and completely ignoring the soil shear strength variation within a layer indicates that the correlation length is infinity, $\theta = \infty$. Meaning, the parameters are perfectly correlated within a layer. The input parameters are probabilistically analyzed from CPT as described in chapter 5 and arranged according to the layer family they represent. The distribution type, the computed mean value, and standard deviation that are representative for each layer are summarized in Table 6.2. Other parameters, soil unit weight, γ_s and attraction, a remain deterministic.

Table 6.2 Plaxis 2D input values of parameters for single random variable approach

<i>Layer</i>	<i>Distribution</i>	μ_ϕ ($^\circ$)	CoV_ϕ
<i>sand</i>	<i>N</i>	<i>36.41</i>	<i>0.15</i>
		μ_{S_u} (KN/m ²)	CoV_{S_u}
<i>Quick Clay</i>		<i>54.52</i>	<i>0.20</i>
<i>Clay</i>	<i>LN</i>	<i>62.25</i>	<i>0.25</i>
<i>Sensitive Clay</i>		<i>94.40</i>	<i>0.25</i>

N – normal distribution, *LN* – lognormal distribution

The geometry and layer stratification remain same as shown in Fig. 6.1. The factor of safety, F_s is analyzed for each 2000 random realization generated using MC sampling method. The output is presented in Fig. 6.3 in histogram plot with the proximate fit of F_s which is normal distribution. The mean value and standard deviation of F_s can easily be obtained from the fitted distribution.

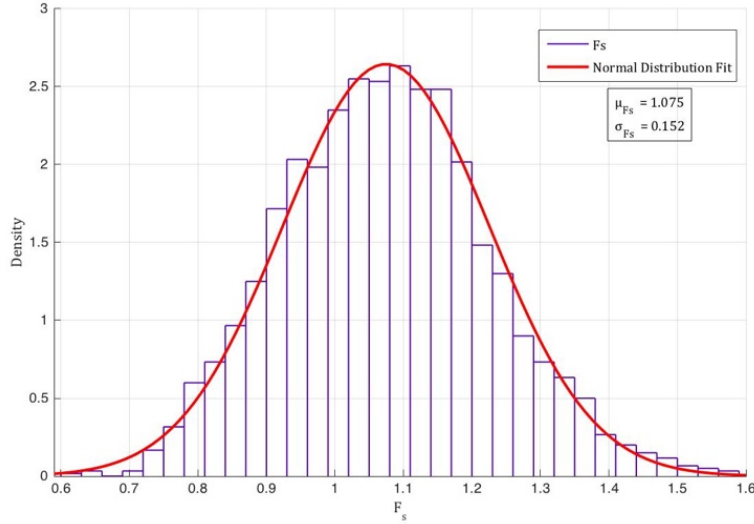


Figure 6.3 Histogram plot and distribution fit of F_s for 2000 MC realizations

After MC realization, the output gives a mean factor of safety, $\mu_{F_s} = 1.075$ with a standard deviation, $\sigma_{F_s} = 0.152$, a minimum value of 0.61 and a maximum 1.59. Fig. 6.3 clearly shows the possibility for F_s to be less than one. This is an indication for the probability that the slope is unsafe and can be described by failure probability, p_f . Since F_s is most likely to be fitted to normal distribution, $F_s \sim N(\mu_{F_s}, \sigma_{F_s})$, the probability of failure, without including any model uncertainty for F_s , can be calculated using the standard normal, Φ transformation:

$$p_f = P(F_s < 1) \quad (6.1)$$

$$p_f = \Phi\left(\frac{1 - \mu_{F_s}}{\sigma_{F_s}}\right) \quad (6.2)$$

p_f is calculated to be 30.1% and can also be spotted on the cumulative density function graph of the representative normally distributed F_s as shown in Fig. 6.4. The p_f can be interpreted as; for the given slope geometry (Rissa Slope), for the range of shear strength parameters assumed, 30 out of 100 similar slopes to be expected to fail at some time during the life of slope, or a length of 30m could be expected to fail in every 100m of slope.

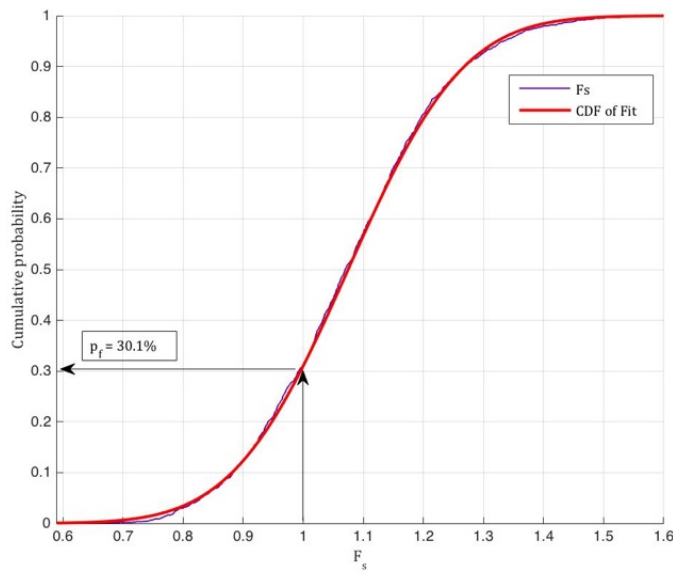


Figure 6.4 Cumulative density function of F_s showing 30.1% probability of failure

6.4 Conditional Random Finite Element Method

CRFEM is a powerful analysis method that accounts for spatially random shear strength parameters and spatial correlation. The inclusion of natural randomness of parameters makes the model much more close to what exists in reality. The software Python(x,y) interface to PLAXIS 2D integrates the probability analysis with finite element analysis and create a CRFEM approach. The probabilistic method accounts for randomness of shear strength. Soil properties are deterministic at measured, but unknown at unobserved locations. The unknown points are estimated from measurements made at a limited number of locations. This is the point where conditional random field is applied. Detail about the conditional random field are presented in Section 3.23. The input to the deterministic finite element model will be conditioned random values assigned by MC sampling method.

6.4.1 Generating Mesh

A computer software, GMSH is used to generate mesh within the entire slope. In CRFEM approach, each and every element is assigned to a specific parametric property based on the probabilistic analysis. So one element possess unique soil property covered by its area to represent the real phenomena. The generated mesh is illustrated in Fig.6.5. Boundary

lines are made centering all the measured locations. The elements inside the boundaries take the observed (measured) values which are probabilistically interpreted in chapter 5. Since each element covers larger area than the CPT measurement reading interval distance, the average of the observed values within an element area is set to be the value of that element. Fine mesh is generated around the observed locations to get more advantage from the observed measurements. Once, all the elements at the observed location assigned to be deterministic, the others will be treated as random variables. The size and the amount of the elements are selected based on the maximum number of random elements that PLAXIS 2D can take. For this particular slope, the generated mesh has 3190 elements.

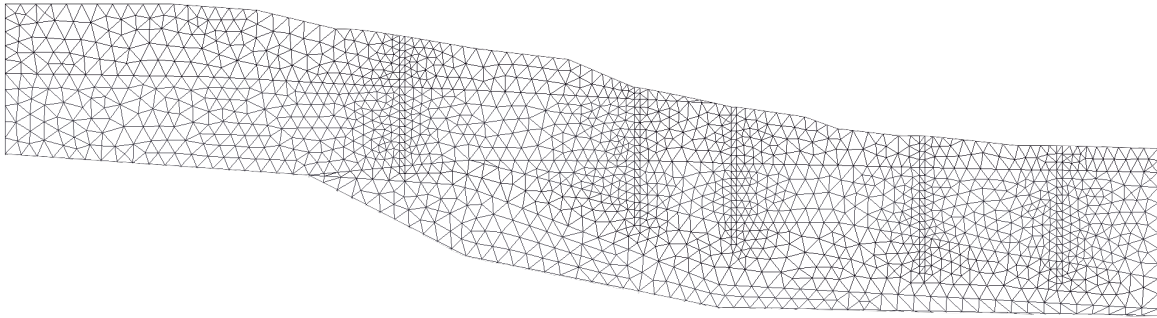


Figure 6.5 Generated mesh diagram with boundary box surrounding CPT profiles

6.4.2 Spatial Length

Horizontal correlation length is not possible to estimate because of the limited data set on horizontal direction. It is known that due to deposition history, the correlation lengths in horizontal direction are longer than in vertical. In this report the effect of the horizontal correlation on factor of safety and failure probability is studied by varying the horizontal correlation length, θ_H to 1m, 15m, 50m, and 100m.

6.4.3 CoV of unobserved elements

The shear strength parameters at unknown points are estimated from measurements made at some limited locations. The estimated values may deviate from the existing reality. To

analyze this deviation effect, simulations have been made by varying the coefficient of variation values of unobserved points.

6.4.4 Local averaging of elements

Characterization of soil parameters are done in a point level. But, in reality, its impossible to achieve a point resolution while making soil measurements. Normally, soil property measurements average the property over the volume incorporated while the measurement is taken. The Rissa Slope is discretized into finite number of elements. In each of these elements, a local averaging process is applied to assign a constant value of shear strength based on the point statistics of the property within the area. Application of local averaging in each element causes a degree of variance reduction and the implementation is made based on PLAXIS 2D scientific manual (Manual).

Numerical integration of area elements

The procedures described in the scientific manual are followed for this study. For 15 node triangle elements, there are two local coordinates, ξ and η with an auxiliary coordinate, $\zeta = 1 - \xi - \eta$. The shape functions for 15 nodes are given in the manual (Manual).

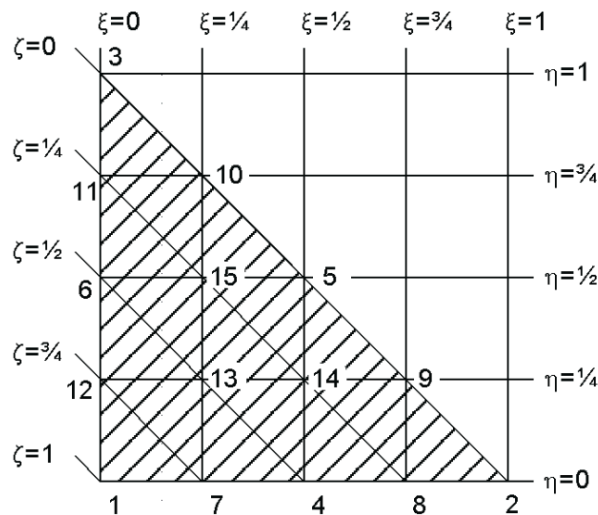


Figure 6.6 Local numbering and positioning of nodes of a 15 - node triangular element

The Gaussian numerical integration over the element area is given as:

$$\iint F(\xi, \eta) d\xi d\eta = \sum_{i=1}^k F(\xi_i, \eta_i) w_i \quad (6.3)$$

Where, $F(\xi_i, \eta_i)$ is a Markov correlation function at position ξ_i and η_i and w_i is the weight factor of point i . For 15 node element, 12 integration points are used. The position and weight factors of the integration points are given in Table 13 (PLAXIS 2D manual).

Table 6.3 Position and weight factor of 12-point integration for 15 - node elements

Points	ξ_i	η_i	ζ_i	w_i
1, 2 & 3	0.063089	0.063089	0.873821	0.050845
4, 5 & 6	0.249286	0.249286	0.501426	0.116786
7...12	0.310352	0.053145	0.636502	0.082851

In general, 7 simulations have been made by using different combination of inputs for unobserved parameters. The local averaging concept is applied only on the seventh simulation due to the complex procedures and the limit of time. The corresponding effect is studied.

The elements at the observed locations being deterministic, for the unobserved elements the input parameters stated in Table 6.4 are used for the first simulation.

Table 6.4 Input values of parameters for unobserved points for simulation 1

	Mean 1	CoV 1	
layer	μ_φ ($^\circ$)	CoV_φ	θ_H (m)
sand	35.4	0.15	50
	μ_{S_u} (KN/m ²)	CoV_{S_u}	
Quick Clay	54.52	0.2	50
Clay	62.25	0.25	50
Sensitive Clay	94.4	0.25	50

θ_H is correlation length in horizontal direction, while Mean 1 and CoV 1 are set of input values for unobserved elements used for simulation 1. For the other simulations, the input parameters are presented in terms of the first simulation as described in Table 6.5.

Table 6.5 Input parameters of unobserved points for all simulations given in terms of simulation 1

Simulations	Mean	CoV	$\theta_H(m)$
Simulation 1	Mean 1	CoV 1	50
Simulation 2	Mean 1	1.5 (CoV 1)	50
Simulation 3	Mean 1	2.0 (CoV 1)	50
Simulation 4	Mean 1	2.0 (CoV 1)	1
Simulation 5	Mean 1	2.0 (CoV 1)	15
Simulation 6	Mean 1	2.0 (CoV 1)	100
Simulation 7 (local averaging)	Mean 1	2.0 (CoV 1)	50

The analysis is made by dividing the simulation into 3 sections. Simulation 1 to 3 is by changing the coefficient of variation of unobserved points. Simulation 3 to 6, by varying the horizontal correlation length. And finally simulation 7 with the application of local averaging.

6.5 Simulation results

The geometry output for simulation1 input is shown in Fig 6.7. The variation in shear strength input can easily be identified by the color difference of the elements. One element, one type of color, has one specific and unique property. In PLAXIS 2D, the assigning of colors to each element is random so that the conditional property and the correlation between elements can not be observed here.

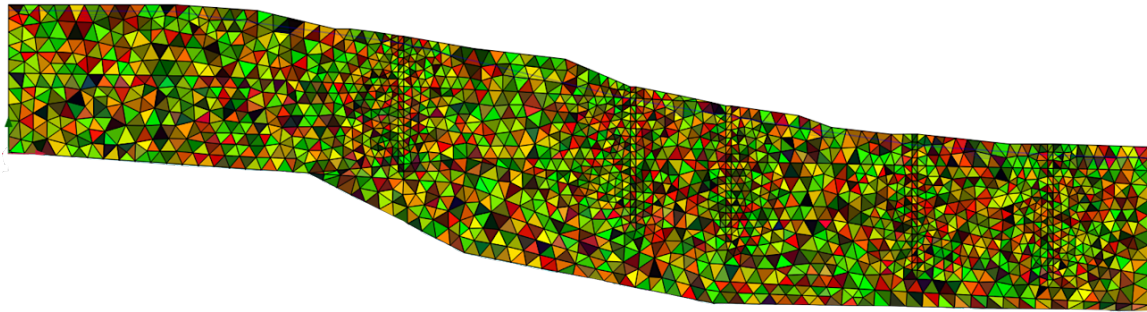


Figure 6.7 Plaxis 2D geometry output of generated random field for simulation 1

The deformation of the Finite Element Mesh at the end of elastic analysis is shown in Fig. 6.8 for the geometry input presented in Fig. 6.7.

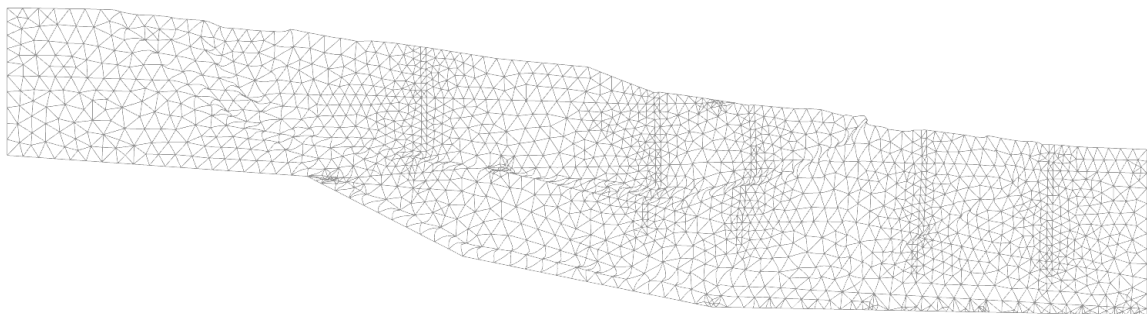


Figure 6.8 Deformed mesh output at the end of elastic analysis

The likely failure mechanism is presented in Fig. 6.9 in terms of deviatoric strain. One of the advantage of CRFEM analysis is, unlike deterministic analysis method all the possible weakest zones accounted for failure are freely detected as shown in Fig. 6.9.

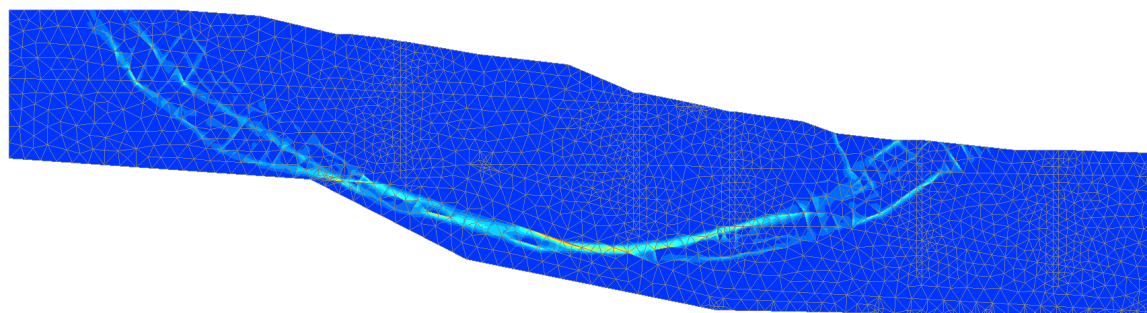


Figure 6.9 Failure mechanism in terms of deviatoric strain for simulation 1

For a given set of input shear strength parameters, Monte Carlo simulations are performed. For each MC realization, the code developed in Python(x,y) overwrites the input values directly on PLAXIS 2D input file package. Similarly, each result is extracted from the output file of PLAXIS 2D exactly after each realization. 1000 realizations are made for each simulation and the corresponding factor of safety, F_s behavior is studied as shown in Fig. 6.10.

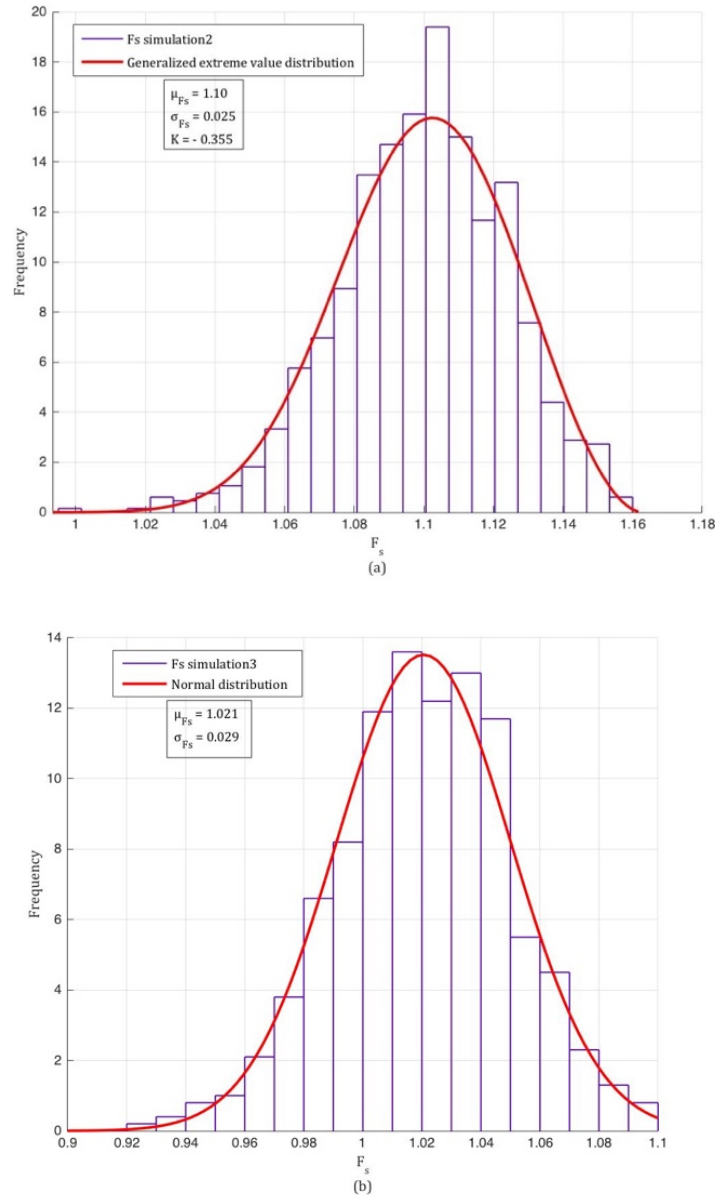


Figure 6.10 Histogram plot and distribution fit of F_s for 1000MC realizations for simulation 2 (a) and simulation 3 (b)

6.5.1 Probability of failure

F_s calculating by FEM is associated with uncertainties due to the estimation capability of design model on the real phenomena. This can be due to geometry of the slope, uncertainty in ground water table or calculation method. By taking all this uncertainties into consideration, model error ϵ_M is introduced to be normally distributed with zero mean and standard deviation = 0.05 (Wu, 2009). The new factor of safety, F_s^* , which includes uncertainties associated with model, can be calculated by:

$$F_s^* = F_s + \epsilon_M \quad (6.4)$$

Failure will be observed when $F_s^* < 1$. The corresponding failure probability, p_f can be expressed by:

$$p_f = P(F_s^* < 1) = P(F_s + \epsilon_M < 1) = P(\epsilon_M < 1 - F_s) \quad (6.5)$$

Dividing both side of the inequality by σ_{ϵ_M} ;

$$p_f = P\left(\frac{\epsilon_M}{\sigma_{\epsilon_M}} < \frac{1 - F_s}{\sigma_{\epsilon_M}}\right) \quad (6.6)$$

Since ϵ_M is normally distributed, $\epsilon_M \sim N(0, \sigma_{\epsilon_M})$, the parameter $\epsilon_M/\sigma_{\epsilon_M}$ follows a standard normal distribution, $\epsilon_M/\sigma_{\epsilon_M} \sim N\left(\mu_{\epsilon_M/\sigma_{\epsilon_M}} = 0, \sigma_{\epsilon_M/\sigma_{\epsilon_M}} = 1\right)$. Therefore, Eqn. 6.6 can be calculated using the standard normal transformation:

$$p_f = \Phi\left(\frac{1 - F_s}{\sigma_{\epsilon_M}}\right) \quad (6.7)$$

For the total number of N realization, the average failure probability is then calculated as:

$$p_f = \frac{1}{N} \sum_{i=1}^N \Phi\left(\frac{1 - F_s}{\sigma_{\epsilon_M}}\right) \quad (27)$$

The adaptation of probability of failure is illustrated below in Fig. 6.11 and Fig. 6.12 for simulation 2 and 3. Keeping the analyzed values of F_s , the normally distributed ϵ_M is randomly generated using $\mu_{\epsilon_M} = 0$ and $\sigma_{\epsilon_M} = 0.05$. The combined effect of $F_s^* = F_s + \epsilon_M$ is then studied.

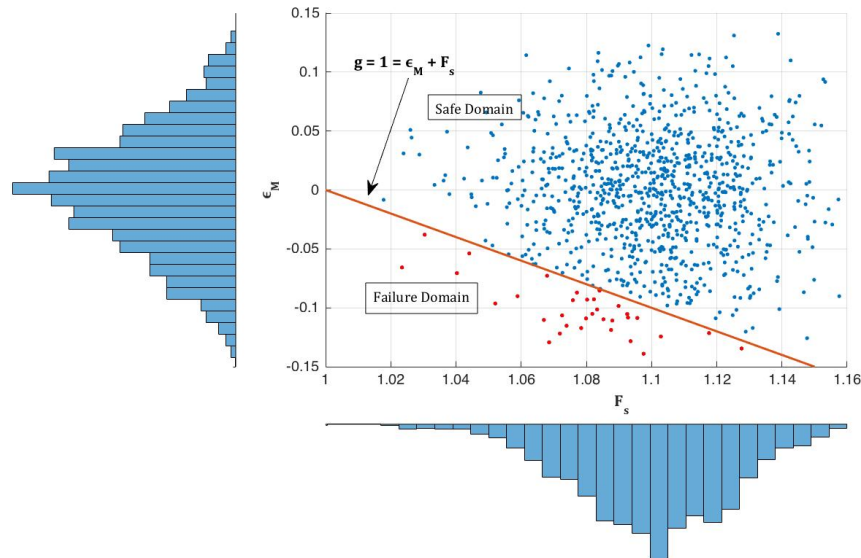


Figure 6.11 Failure probability realization including the effect of model uncertainty for simulation 2 (CoV = 1.5 CoV1)

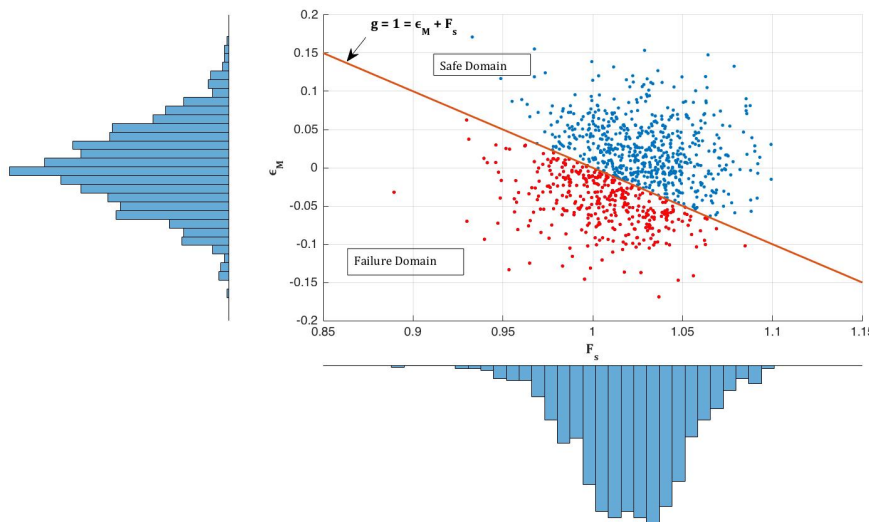


Figure 6.12 Failure probability realization including the effect of model uncertainty for simulation 3 (CoV = 2 CoV1)

The function $g = 1 = F_s + \epsilon_M$, is a limit state boundary that separates the safe and unsafe domain and also assess the performance of the slope stability. It has positive value ($g - 1 > 0$) when the slope is safe and non-positive value ($g - 1 < 0$) when the slope is unsafe. The failure probabilities calculated for all simulations using Eqn. 6.4 – 6.8 are summarized in the Table 6.6.

Table 6.6 Mean value for F_s and probability of failure for simulation 1-7

Simulations	μ_{F_s}	σ_{F_s}	p_f
Simulation 1	1.153	0.020	0.24%
Simulation 2	1.100	0.025	3.66%
Simulation 3	1.020	0.030	36.00%
Simulation 4	1.029	0.019	29.43 %
Simulation 5	1.029	0.024	29.47%
Simulation 6	1.025	0.031	33.45%
Simulation 7	1.120	0.015	1.08%

6.5.2 The effect of CoV

To analyze the effect CoV, in simulations 1, 2 & 3 the coefficient of variation values of unobserved parameters are sated up to be CoV1, 1.5 (CoV1), 2 (CoV1) respectively with same mean, Mean 1. The exact numerical figures are presented in Table 6.4 and 6.5. The corresponding output is summarized in Fig. 6.13. It is expected that for every increase in coefficient of variation of the input parameters, there will be an increase in variability of the output, F_s . This is due to the fact that for high range of CoV (keeping the mean unchanged), the MC sampling technique can freely move within relatively large range and make different sample combination of the inputs that results a relatively more fluctuating output or increase in standard deviation. Similarly, when the CoV of input parameters decrease, the resulted F_s s will get relatively more concentrated around the mean as shown in Fig. 6.13. Its is also shown in the figure that, for higher values of CoV, the mean value of F_s will decreases and results higher failure probability. This can be because of the strength domination effect of weaker elements in the distribution for this particular slope.

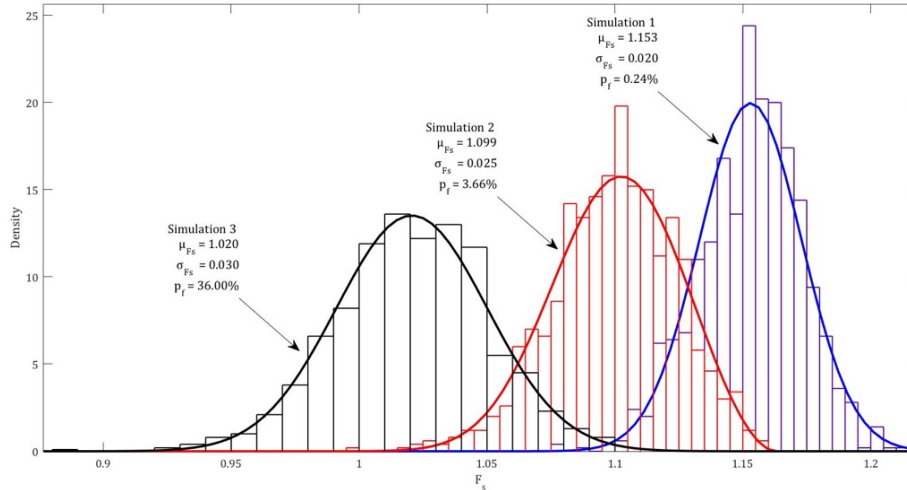


Figure 6.13 The effect of CoV on F_s and p_f for simulations 1, 2 and 3

Normal distribution is best fit for simulation 1 and 3 while simulation 2 is most likely to follow generalized extreme value distribution with an extending left tail.

6.5.3 The effect of horizontal correlation length

The effect of horizontal correlation length is studied from simulation 4, 5 and 6, having horizontal correlation length 1m, 15m and 100m respectively. To get a good effect of θ_H over p_f , 2 (CoV 1) is used for the simulations with the same mean, Mean1. The output of F_s is shown in Fig 6.14 as a histogram plot with the corresponding distribution fit.

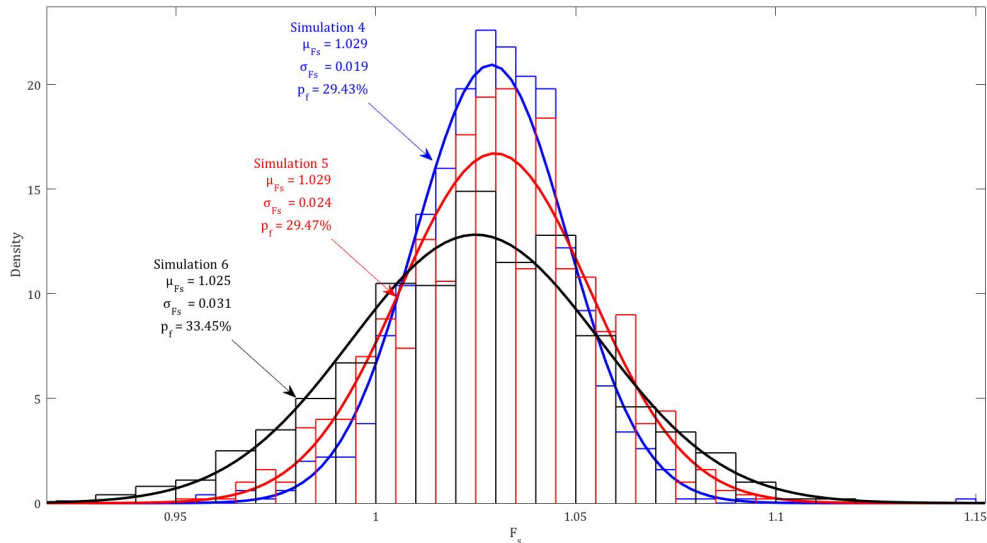


Figure 6.14 The effect of horizontal correlation length on F_s and p_f for simulations 4, 5 and 6 ($\theta_H = 1m, 15m$ and $100m$ respectively)

As shown in Fig. 6.14, the increase in horizontal correlation length does not affect the mean value of the factor of safety. But for this particular case study, it increases the standard deviation of F_s , which follows increase in probability of failure. The increase in θ_H does not have much effect on p_f for the first two simulations ($\theta_H = 1m$ and $15m$). But, when extending θ_H further to $\theta_H = 100m$, p_f increases significantly. When the correlation length increases to positive infinity, the parameters will become perfectly correlated, and the random finite element approach will convert to single random variable approach, SRV. Fig. 6.14 also shows that, for every decrease in standard deviation of F_s , the the peak height of the curve increases. This is to fulfill the criteria of probability density function, that states, the area under the curve is always unity. Therefore, the peak extends higher to compensate the loss in area due to decrease in standard deviation and makes the area unity.

6.5.4 Effect of local averaging

The procedure of local averaging is implemented for the same input parameters of simulation 3 and the effect is shown in Fig. 6.15 as simulation 7.

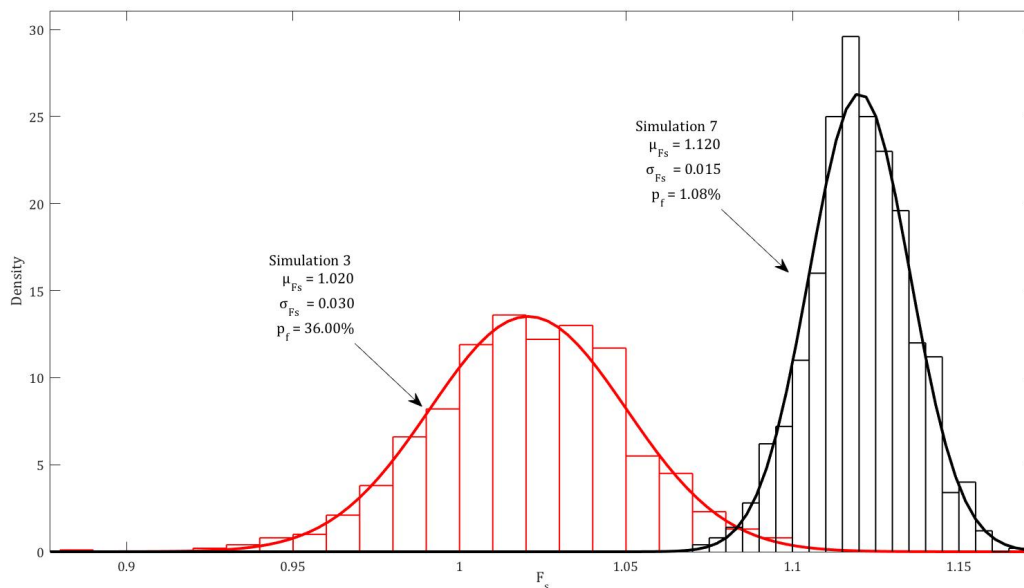


Figure 6.15 The effect of local averaging, simulation 7 on F_s and p_f implemented on simulation 3

The main effect of local averaging is reduction in variance of input parameters, which causes the reduction in standard deviation of F_s . This reduction of variance depends on the size of the random field discretization (element size). The bigger the element size, the higher the variance reduction will be. Fig. 6.15 shows that the standard deviation of simulation 7 (0.015) is half of simulation 3 (0.030). This relatively low variability in the results is because of the random field discretization being not fine enough. This results in a significant variance reduction in the input parameters and correspondingly reduction in the variability of the calculated factor of safety. Beside the variability, mean value of F_s is also increased from 1.02 to 1.12 and results very low failure probability. This can be due to the variance reduction in the input parameters, the effect of weaker elements is reduced in the distribution for this particular slope.

Chapter 7

Discussions

The over all procedure followed in this thesis are categorized in to three main parts. The sections can be classified into; uncertainty quantification and probabilistic interpretation of parameters, conditional random field generation and sampling technique, output probability density function of F_s and failure probability. The overall scheme of these sections can be summarized in Fig. 7.1.

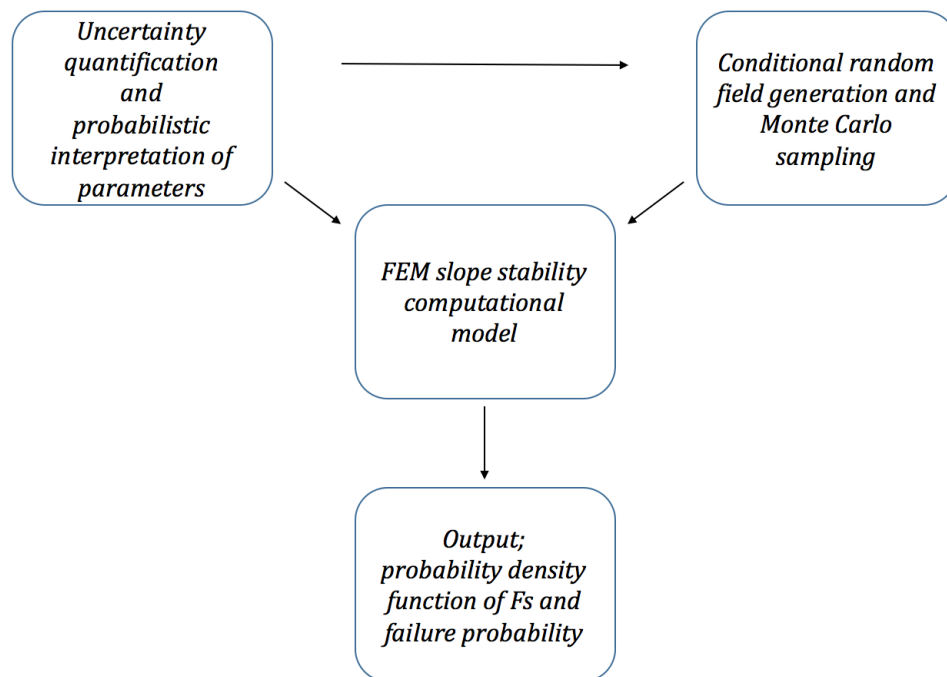


Figure 7.1 Overall procedure for application of advanced probabilistic slope stability analysis

7.1 Uncertainty and parameters interpretation

7.1.1 Spatial variability

The main part of reliability analysis is modelling of uncertainty. Uncertainty may arise because of limited information or limited number of observations on the studied variable, form imperfection of measuring equipment, fault in measurement procedure, or due to the estimation capability of design model on the real phenomena.

Quantitative characterization and reduction of uncertainties are executed through the knowledge of probability theory and statistical analysis. Such modeling of uncertainty increases the confidence on the estimation of the corresponding likelihood of certain outcome.

Spatial variability of soil parameters can be modeled by random field theory. For this study, corrected tip resistance from CPT measurement is studied as random field. Correlation length is one of the parameters that represent spatial variability of soil. Maximum likelihood method is used to estimate the vertical correlation length, trend mean value and standard deviation of corrected tip resistance for each profile on Rissa slope, section 3-3. Likelihood function is a function of mean, standard deviation and correlation length so that it identifies the values of the properties, that make the likelihood function a maximum.

7.1.2 Probabilistic interpretation of parameters

Factor of safety in slope stability analysis can be defined as the ratio between average shear strength of the soil, τ_f to the average mobilized shear stress developed along the potential failure surface, τ_{mob} ($F_s = \frac{\tau_f}{\tau_{mob}}$). Therefore, the main parameter in slope stability analysis is shear strength of the soil. That is, undrained shear strength for clay soils, and friction angle for sand. To implement the advanced probabilistic slope stability analysis, these shear strength parameters are needed to pass through two steps. The first one is, creating a link between the strength parameters and the corrected tip resistance from CPT measurement. Secondly, constructing a probabilistic interpretation of strength parameters which

accounts for uncertainties of the measured values. Both processes are described in detail in chapter 5.

7.2 Conditional random field

In advanced probabilistic slope stability approach, each element in the generated mesh takes one unique shear strength property. Conditional random field is the techniques used to facilitate this assigning process.

Once the shear strength parameters are probabilistically interpreted in measured locations, the parameters at unknown points are estimated from those known values by generating conditional random field. The main concept behind is, elements which are near to measured locations will possess similar property to the observed values than those which are far away. This property of conditional random field is shown in Fig. 7.2. The PLAXIS 2D output is assigned to display the mean values of the elements.

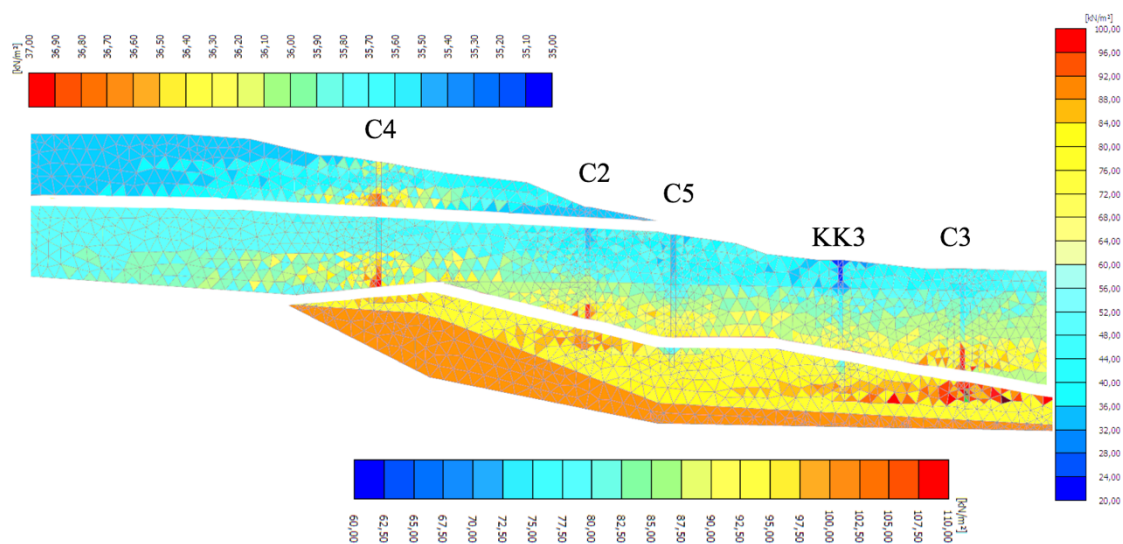


Figure 7.2 Conditionality effect on the generated random field for simulation 3

The elements within the boundary box centering the measured location, are assigned measured values that are probabilistically interpreted from corrected tip resistance of CPT. For the others, conditional random field is generated and the effect of conditionality is clearly shown in Fig. 7.2. The elements next to the boundary box have the same or nearly same

color as elements within the box (observed elements) and the effect will decrease (change in color will observe) when the unobserved elements get far and far away from the observed elements. In other words, when the distance between an observed and an unobserved element increases, the correlation and link between these elements will decrease and for fairly enough separation distance, the unobserved element will be treated as random field without conditionality. These is the effect of conditional random field with correlation length. In Fig. 7.2, to get a clear view of the color differences, the slope is divided into three sections by varying the color legend and for each section, the color legend is presented next to the sectioned piece.

7.2.1 Monte Carlo sampling

In the application of conditional random field, Monte Carlo sampling technique is used to generate sequence of random numbers. The generating process is guided by the distribution type, mean value and standard deviation of the random field parameters. Monte Carlo sampling has two advantages which makes it preferable for this study. First, its simple and straight forward to apply and doesn't require detail knowledge of probability theory. The second reason is, compared to other sophisticated sampling techniques, it does not take much calculation time.

For each conditional random finite element simulation, 1000 MC realization is assumed to be enough to give reliable and reproducible estimate of failure probability. Normally, total number of realization can be estimated for the required coefficient of variation of failure probability which in most cases given by $CoV(p_f) < 0.1$. The coefficient of variation of the estimate for number of realization, N_s can be calculated as:

$$CoV(p_f) = \sqrt{\frac{1 - p_f}{N_s p_f}} \quad (7.1)$$

The highest failure probability calculated in this study is occurred during simulation 3 with a value of 36% as described in Table 6.6. The corresponding CoV is then calculated using Eq. 7.1 and gives a value, $CoV(p_f) = 0.042$ which is in the acceptable range.

7.3 Factor of safety and failure probability

Three different slope stability analysis methods are implemented on Rissa Slope. Initially, the slope is investigated using traditional approach with a constant, one deterministic value for each soil layer. Simple probabilistic concept is then implemented with single random variable technique. Finally, different simulations have been made using CRFEM approach. For comparison of the methods, the result from all three methods, for nearly equivalent input values of parameters are shown in Table 7.1.

Table 7.1 Comparison between deterministic, SRV and CRFEM approaches

Methods	μ_{F_s}	σ_{F_s}	p_f
Deterministic	1.022	-	-
SRV	1.075	0.152	30.1%
CRFEM	1.153	0.020	0.24%

The traditional deterministic approach provides only one factor of safety value for the corresponding single value input, without any further information. This value is less than the other two methods. There is a result difference between the SRV and CRFEM approach. The main reason for this particular case is, SRV approach underestimates the shear strength parameters of the soil while representing the whole soil layer with one single value. In addition, one single value input with relatively high variation, increases the output variability, σ_{F_s} followed by raise in failure probability as shown in Table 7.1.

CRFEM is effected for different input values of unobserved parameters using a number of different simulations. First three simulations are made by changing the coefficient of variation for unobserved location. The results are described in detail in section 6.5.2. In here, the corresponding effect on failure probability for the changes in CoV is plotted as shown in Fig.7.3.

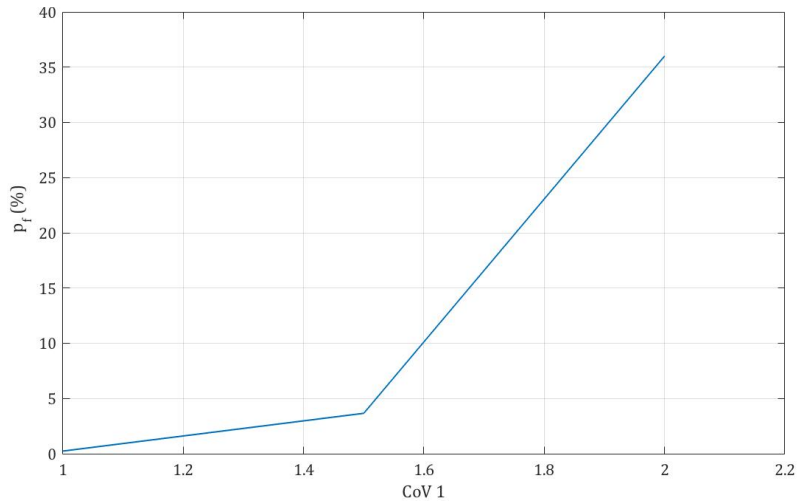


Figure 7.3 Relation between coefficient of variation and probability of failure

Since the slope is combination of different layers, the increment in CoV is made in terms of the first simulation input which is $CoV1$. The figure clearly shows that the increase in CoV increases the failure probability. this is due to the effect that, for each increase in CoV , weaker elements dominate the strength in the distribution for this particular slope.

The next three simulations are made by changing the horizontal correlation length. The results are described in detail in section 6.5.3. In here, the corresponding effect on failure probability for change in horizontal correlation length is plotted as shown in Fig.7.4.

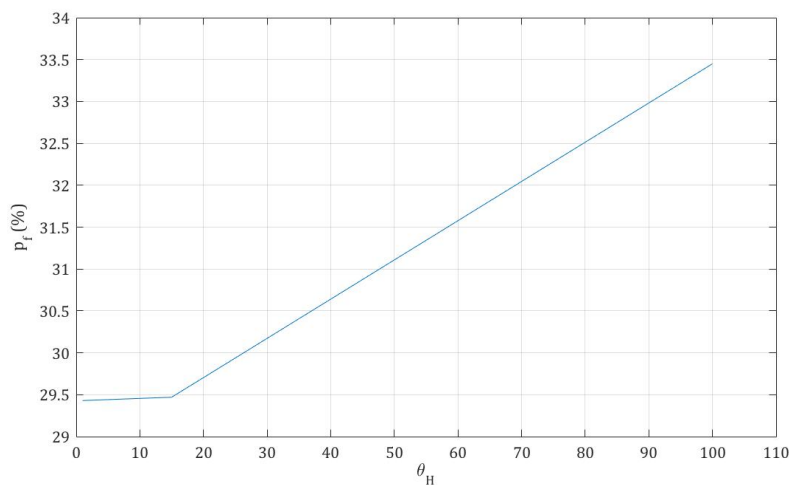


Figure 7.4 Relation between horizontal correlation length and probability of failure

7.3 Factor of safety and failure probability

The increase in θ_H does not show much effect on p_f for the first two simulations ($\theta_H = 1m$ and $15m$). But when extending θ_H further to $\theta_H = 100m$, p_f increases significantly.

Finally, the concept of local average is applied on Rissa slope. The main consequence of local average is variance reduction which causes reduction in the variability of the calculated factor of safety. The resulted output can also be described similarly as the effect of *CoV* reduction.

All and all, the CRFEM results show that the inclusion of local averaging, reduction in *CoV* and horizontal correlation length will lead to a smaller probability of failure for the particular case, Rissa.

Chapter 8

Conclusions and recommendations

8.1 Conclusions

Geotechnical design is traditionally based on deterministic analysis using global or partial safety factors to take soil variability into account and does not give a complete indication of the safety margin. These traditional approaches are mainly based on experience or expert judgment and does not explicitly account for the effect of uncertainties in soil parameters. Therefore, the safety margins should be assessed within a mathematical framework by using probabilistic methods to evaluate the probability of failure. One of the most important issues in geotechnical design is the quantification of soil variability. Variability in soil properties, uncertainty in measurements, uncertainty in analysis models etc. all contribute to a failure probability (Veritas, 1992). It is not possible to completely remove uncertainties. But, such advanced probabilistic approaches provide a way to handle the uncertainty in a controlled manner and give a reliable way to calculate probability of failure.

Probabilistic analysis is powerful in investigating the influence of uncertainties on a given geotechnical problem. The way to conduct an uncertainty quantification in geotechnical engineering is shown in a particular case study, Rissa slope. Advanced probabilistic slope stability analysis is conducted to calculate the factor of safety and failure probability of Rissa slope. Probabilistic assessments are made to study the relative influence of variability and spatial correlation. To account for uncertainties, interpretations of soil properties are made based on a probabilistic link between the CPT data and soil parameters. Accounting for uncertainties while determining soil parameters brought confidence in predicting the

output behavior. Conditional random field is generated to characterize spatial variability of soil parameters. Lastly, the potential of the framework of uncertainty quantification, the effects of spatial soil variability and local averaging are realized by conducting probabilistic analysis with a Monte Carlo sampling technique.

All in all, this case study shows the effect of soil variability, spatial variability, and local averaging at different scales for the random input parameters.

It is also very important to be aware of the limitations that lie in a probabilistic analysis. Geostatistical evaluation in geotechnical parameters are difficult to make due to the limitation of the available data from ground investigation. In order to make probabilistic analysis, one should be aware of the need for bigger investigation campaign. Beside this, in applied engineering, probabilistic concepts are not adapted because of the deficiency in statistical background knowledge that is needed to understand the result of probabilistic analysis.

In conclusion, within chapter 2 the basic theoretical background that are a base for initiating the advanced probabilistic approach are presented. The basics of safety and uncertainty are summarized in chapter 3. Chapter 4 concentrates on the characterization of the case study area and summarize the available measured values from the ground investigation, CPT. Uncertainty quantification and probabilistic interpretation of parameters are developed in chapter 5. The the results and discussion of advanced probabilistic approach are presented in chapter 6 and 7. These case study shows the application of uncertainty quantification and shall guide the reader to a comprehensive understanding of the presented approaches.

8.2 Recommendations for further work

Probabilistic approach is a wide and more of a subjective topic. It can be extended unlimitedly and can be made more sophisticated. In this study, only shear strength parameters are taken as random variables because of time limitation. However, it is possible to further extend the amount of random variables in the advanced probabilistic slope stability analysis by considering geometry of the slope, boundary of soil layers, height of ground water table,

and other soil parameters to be random. This is expected to give more accurate estimation for the reliability analysis. The contribution of each random parameter for the probability of failure can also be studied with sensitivity analysis.

The other perception worth mentioning for future work is the integration of Bayesian updating concept while assigning distribution type for the parameters. Application of Bayesian inference identifies the actual range of distribution of the parameter in the probability distribution function. This is expected to reduce the domain range for the sampling algorithms so that reduction in variability of the outputs will follow.

Finally, there are more sophisticated sampling techniques than MC simulation method. As a proposition for further work, it would be interesting to apply the more effective sampling method on the advanced slope stability analysis.

Bibliography

- Al-Awkati, Z. A. (1975). On problems of soil bearing capacity at depth, PhD thesis. *International Journal of Rock Mechanics and Mining Sciences & Geomechanics Abstracts*, 14, A79.
- Army, U. (2003). Engineering Manual. Engineering and design-Slope stability. *US Army Corps of Engineering*.
- Baecher, G. B., & Christian, J. T. (2005). *Reliability and statistics in geotechnical engineering*: John Wiley & Sons.
- Bromhead, E. (2006). *The stability of slopes*: CRC Press.
- Craig, R. F. (2004). *Craig's soil mechanics*: CRC Press.
- Dudley, R. M. (1999). *Uniform central limit theorems* (Vol. 23): Cambridge Univ Press.
- Duncan, J. M., Wright, S. G., & Brandon, T. L. (2014). *Soil strength and slope stability*: John Wiley & Sons.
- Durgunoglu, H. T., & Mitchell, J. K. (1973). Static penetration resistance of soils.
- Fell, R., MacGregor, P., Stapledon, D., & Bell, G. (2005). *Geotechnical engineering of dams*: CRC Press.
- Fenton, G. A., & Griffiths, D. V. (2008a). Estimation Risk Assessment in Geotechnical Engineering (pp. 161-201): John Wiley & Sons, Inc.
- Fenton, G. A., & Griffiths, D. V. (2008b). Random Fields Risk Assessment in Geotechnical Engineering (pp. 91-125): John Wiley & Sons, Inc.
- Fenton, G. A., & Griffiths, D. V. (2008c). Review of Probability Theory Risk Assessment in Geotechnical Engineering (pp. 1-69): John Wiley & Sons, Inc.
- Fenton, G. A., & Griffiths, D. V. (2008d). Slope Stability Risk Assessment in Geotechnical Engineering (pp. 381-400): John Wiley & Sons, Inc.
- Gregersen, O. (1981). The quick clay landslide in Rissa, Norway *The sliding process and discussion of failure modes*. NGI, publication No. 135 Oslo 1981.

- Harris, J. W., & Stöcker, H. (1998). *Handbook of mathematics and computational science*: Springer Science & Business Media.
- ISSMGETC32. (July, 2004). Risk Assessment - Glossary of Terms *Technical Committee on Risk Assessment Managment*.
- Kellet, J. (2014). Disaster risk reduction makes development sustainable.
- Kornbrekke, H. A. (2012). Skråningsstabilitet ved Rein Kirke med utgangspunkt i resultater fra Sherbrooke blokkprøver.
- Kulhawy, F., & Carter, J. (1992). Settlement and bearing capacity of foundations on rock masses. *Engineering in rock masses*, 231-245.
- Kulhawy, F. H., & Mayne, P. W. (1990). *Manual on Estimating Soil Properties for Foundation Design*. Cornell University. Geotechnical Engineering Group: Electric Power Research Institute.
- Lacasse, S., & Nadim, F. (1997). Uncertainties in characterising soil properties. *Publikasjon-Norges Geotekniske Institutt*, 201, 49-75.
- Lunne, T., Robertson, P., & Powell, J. (1997). Cone penetration testing. *Geotechnical Practice*.
- Manual, S. PLAXIS 2D-Version8; Edited by RBJ Brinkgreve. *Delft University of Technology & PLAXIS bv; The Netherlands*.
- Nadim, F. (2007). Tools and Strategies for Dealing with Uncertainty in Geotechnics. In D. V. Griffiths & G. A. Fenton (Eds.), *Probabilistic Methods in Geotechnical Engineering* (Vol. 491, pp. 71-95): Springer Vienna.
- Noce, T. E. (2003). *Subsurface exploration with the cone penetration testing truck [electronic resource] / Thomas E. Noce and Thomas L. Holzer*. [Reston, Va.]: U.S. Dept. of the Interior, U.S. Geological Survey.
- Phoon, K.-K., & Kulhawy, F. H. (1999). Characterization of geotechnical variability. *Canadian Geotechnical Journal*, 36, 612--624. doi:10.1139/t99-038
- Robertson, P. K., & Campanella, R. (1986). *Guidelines for Use, Interpretation and Application of the CPT and CPTU*: Hogentogler & Company.
- Robertson, P. K., & Campanella, R. G. (1983a). Interpretation of cone penetration tests. Part I: Sand. *Canadian Geotechnical Journal*, 20, 718--733.

- Robertson, P. K., & Campanella, R. G. (1983b). Interpretation of cone penetration tests. Part II: Clay. *Canadian Geotechnical Journal*, 2019, 734--745.
- Schmertmann, J. H. (1975). *Measurement of in situ shear strength*. Paper presented at the In Situ Measurement of Soil Properties.
- Senneset, K., & Janbu, N. (1985). Shear strength parameters obtained from static cone penetration tests *Strength Testing of Marine Sediments: Laboratory and In-situ Measurements*: ASTM International.
- Veritas, N. (1992). *Structural reliability analysis of marine structures*: Det Norske Veritas.
- Vesic, A. B. (1963). Bearing capacity of deep foundations in sand. *Highway research record*(39).
- Wu, T. H. (2009). *Reliability of geotechnical predictions*. Paper presented at the Proc. of The Second International Symposium on Geotechnical Risk and Safety.